



# Effect of Lockdown on Pollutant Levels in the Delhi Megacity: Role of Local Emission Sources and Chemical Lifetimes

Chinmay Mallik<sup>1\*</sup>, Harish Gadhavi<sup>2</sup>, Shyam Lal<sup>2</sup>, Rahul Kant Yadav<sup>1</sup>, R. Boopathy<sup>3</sup> and Trupti Das<sup>3</sup>

<sup>1</sup>Department of Atmospheric Science, Central University of Rajasthan, Ajmer, India, <sup>2</sup>Physical Research Laboratory, Ahmedabad, India, <sup>3</sup>Environment and Sustainability Department, CSIR-Institute of Minerals and Materials Technology, Bhubaneswar, India

## OPEN ACCESS

### Edited by:

Suvarna Sanjeev Fadnavis,  
Indian Institute of Tropical  
Meteorology (IITM), India

### Reviewed by:

Rohini Bhawar,  
Savitribai Phule Pune University, India  
Sabine Griesbach,  
Julich-Forschungszentrum,  
Helmholtz-Verband Deutscher  
Forschungszentren (HZ), Germany

### \*Correspondence:

Chinmay Mallik  
chinmay.mallik@curaj.ac.in

### Specialty section:

This article was submitted to  
Atmosphere and Climate,  
a section of the journal  
Frontiers in Environmental Science

**Received:** 19 July 2021

**Accepted:** 10 September 2021

**Published:** 13 October 2021

### Citation:

Mallik C, Gadhavi H, Lal S, Yadav RK,  
Boopathy R and Das T (2021) Effect of  
Lockdown on Pollutant Levels in the  
Delhi Megacity: Role of Local Emission  
Sources and Chemical Lifetimes.  
*Front. Environ. Sci.* 9:743894.  
doi: 10.3389/fenvs.2021.743894

The COVID-19 pandemic resulted in changed emission regimes all over the world. India also imposed complete lockdown on all modes of travel and industrial activities for about 2 months from 25-March-2020 and later unlocked these activities in a phased manner. Here, we study signatures of emissions changes on levels of atmospheric trace gases and aerosols contributing to air pollution over multiple sites in India's capital Delhi covering various lockdown and unlock phases using satellite data and *in-situ* observations. The resulting changes in the levels of these species were compared with respect to their average of 2015–2019 to attribute for year to year and seasonal changes. A clear impact of lockdown was observed for AOD, PM, NO<sub>2</sub>, CO, and SO<sub>2</sub> as a result of emission changes, while changed precursor levels led to a change in O<sub>3</sub> chemical regimes impacting its concentrations. A detailed analysis of FLEXPART trajectories revealed increased PM levels over Delhi in north-westerly air masses sourced to Punjab region all the way up to Pakistan. Changes in aerosols and NO<sub>2</sub> were not only restricted to the surface but transcended the total tropospheric column. The maximum decrease in PM, NO<sub>2</sub>, CO, and SO<sub>2</sub> was observed during the month of total lockdown in April. The lockdown impact varied with species e.g., PM<sub>10</sub> and PM<sub>2.5</sub> as well as locations even within the periphery of Delhi. While surface level aerosols and NO<sub>2</sub> showed significant and almost similar changes, AOD showed much lower decrease than tropospheric column NO<sub>2</sub>.

**Keywords:** trace gases, aerosols, lockdown, ozone chemistry, tropospheric NO<sub>2</sub>, FLEXPART trajectories

## INTRODUCTION

Delhi is known for its high levels of air pollution with increasing emissions from various anthropogenic sources. Apart from local, anthropogenic emissions, Delhi's air quality is also impacted by transport of pollutants from the nearby industrial and agricultural sources. Transport of pollutants from the agriculture residue burning both toward the end of autumn and spring in the nearby states of Punjab and Haryana is a regular feature every year. Planning effective strategies for controlling the levels of pollutants needs accurate emission inventories of various sources. The COVID-19 pandemic in India is part of the worldwide pandemic of coronavirus disease 2019 (COVID-19) caused by severe acute respiratory syndrome coronavirus 2 (SARS-CoV-2). The COVID-19 containment effort such as countrywide lockdown provided a unique opportunity to study how pollutant levels change in an

**TABLE 1** | Various phases of lockdown in India to arrest the spread of the infection due to COVID-19.

Type	Duration	Details
Janata Curfew	22 March, 2020 (Sunday)	All activities totally closed
Phase 1	25 March–14 April, 2020 (21 days)	All activities totally closed except emergency services
Phase 2	15 April–3 May, 2020 (19 days)	All activities totally closed except emergency services, essential items
Phase 3	4 May–17 May, 2020 (14 days)	All activities totally closed with some relaxation for limited transport services, interstate trucks for essential items etc.
Phase 4	18 May–31 May, 2020 (14 days)	All activities totally closed except emergency, limited domestic air travel started on 25th May
Phase 5	Unlock phase 1: 1–30 June, 2020 (30 days)	Most of the activities allowed except in highly affected areas. Shopping malls, religious places, hotels, and restaurants allowed to reopen from 8 June. Educational institutions and cinema halls remained closed. No metro train service
Phase 6	Unlock phase 2: 1–31 July, 2020 (31 days)	Lockdown measures were only imposed in containment zones. In all other areas, most activities were permitted. Night curfews were effective only from 10 p.m. to 5 a.m. Intra- and inter-state travel was allowed. International travel remained closed except for limited travel as part of the Vande Bharat Mission. Educational institutions and cinema halls remained closed. No metro train service

otherwise highly polluted urban atmosphere following a curb in various anthropogenic emission sources. While this pandemic started in November 2019 in China, India saw the first case of COVID-19 on January 30, 2020 and the first reported death on March 12 (Andrews et al., 2020; <sup>1</sup>). Henceforth, the infection rate continued to increase. A single-day trial lockdown was announced in India on March 22, followed by the first phase from March 25 and later various other phases for lockdown followed by phasewise unlock as detailed in **Table 1** <sup>2,3</sup>. There are various studies related to the impact of lockdown on pollutant levels in different parts of the world (Le et al., 2020; Sicard et al., 2020; Xu et al., 2020) as well as in India (Dhaka et al., 2020; Jain and Sharma 2020; Mahato et al., 2020; Singh et al., 2020; Nath et al., 2021; Panda et al., 2021). Although this was a nationwide lockdown but we chose to study the impact over Delhi as it is the most polluted major urban region in India. This article provides a detailed account of the changes until almost the end of the government-enforced planned lockdown/unlock periods in 2020 and with respect to emission sources and lifetimes using surface-based *in situ* measurements as well as satellite-based measurements.

## MATERIALS AND METHODS

### The Study Locations

For the present analysis, we have focused on the Delhi metropolitan region (28.20–28.71°N, 77.17–77.38°E). The reasons are that Delhi is a megacity and home to a population of 29 million estimated in 2018 and projected to be the world's most populous in a decade<sup>4,5</sup>. With an area of approximately

1,500 square kilometers, a population density of approximately 19,400 per square km, and being the capital city of India, Delhi is also a hub of connection with close to 11 million vehicles daily plying the roads of Delhi with a growth rate of 5% in 2018<sup>6,7</sup>. Apart from that, Delhi also witnesses a significant flux of industrial emissions including the power plants. The Delhi-Mumbai industrial corridor is one of the biggest in the world. Additionally, a significant amount of pollution in Delhi is attributed to adjoining agriculture waste burning emissions (Perrino et al., 2011; Rajput et al., 2014). Emissions and air pollution were also found to impact the vertical temperature structure over Delhi, leading to accelerated warming (Mallik and Lal, 2011). So, when the COVID-19 was announced and the entire functioning transport system came to a halt suddenly, the impacts were expected to be significant. To understand the impact of lockdown on the emissions and the subsequent impact of these changed emissions as a result of enforcement of various lockdown/unlock phases on atmospheric concentrations of particulate matter (PM: 10 and 2.5), nitrogen dioxide (NO<sub>2</sub>), ozone (O<sub>3</sub>), carbon monoxide (CO), and sulphur dioxide (SO<sub>2</sub>), we have analyzed the respective data from six different locations in Delhi. These locations are given in **Table 2** and are also shown in **Figure 1**. The study sites are: Anand Vihar (AnVh), Punjabi Bagh (PnBg), Shadipur (SdPr), Central Road Research Institute (CRRI), NSIT Dwarka (NstD), and EPA/US Embassy Delhi (EPA-D).

Anand Vihar is a posh locality in the Eastern part of Delhi with many residential colonies and shopping complexes. It harbors a major railway station and is situated in the east of the River Yamuna. The major emission sources in this region are likely to be the residential and traffic sectors. However, in the western part, there are a few industries manufacturing paper, glass, and chemicals. While paper industries can be a secondary source

<sup>1</sup><https://archive.pib.gov.in/archive2/erelease.aspx> (Release IDs: 200168 & 200237)

<sup>2</sup><https://www.mha.gov.in/notifications/circulars-covid-19>

<sup>3</sup>[https://www.mha.gov.in/sites/default/files/MHAorder%20copy\\_0.pdf](https://www.mha.gov.in/sites/default/files/MHAorder%20copy_0.pdf)

<sup>4</sup><https://www.populationu.com/in/delhi-population>

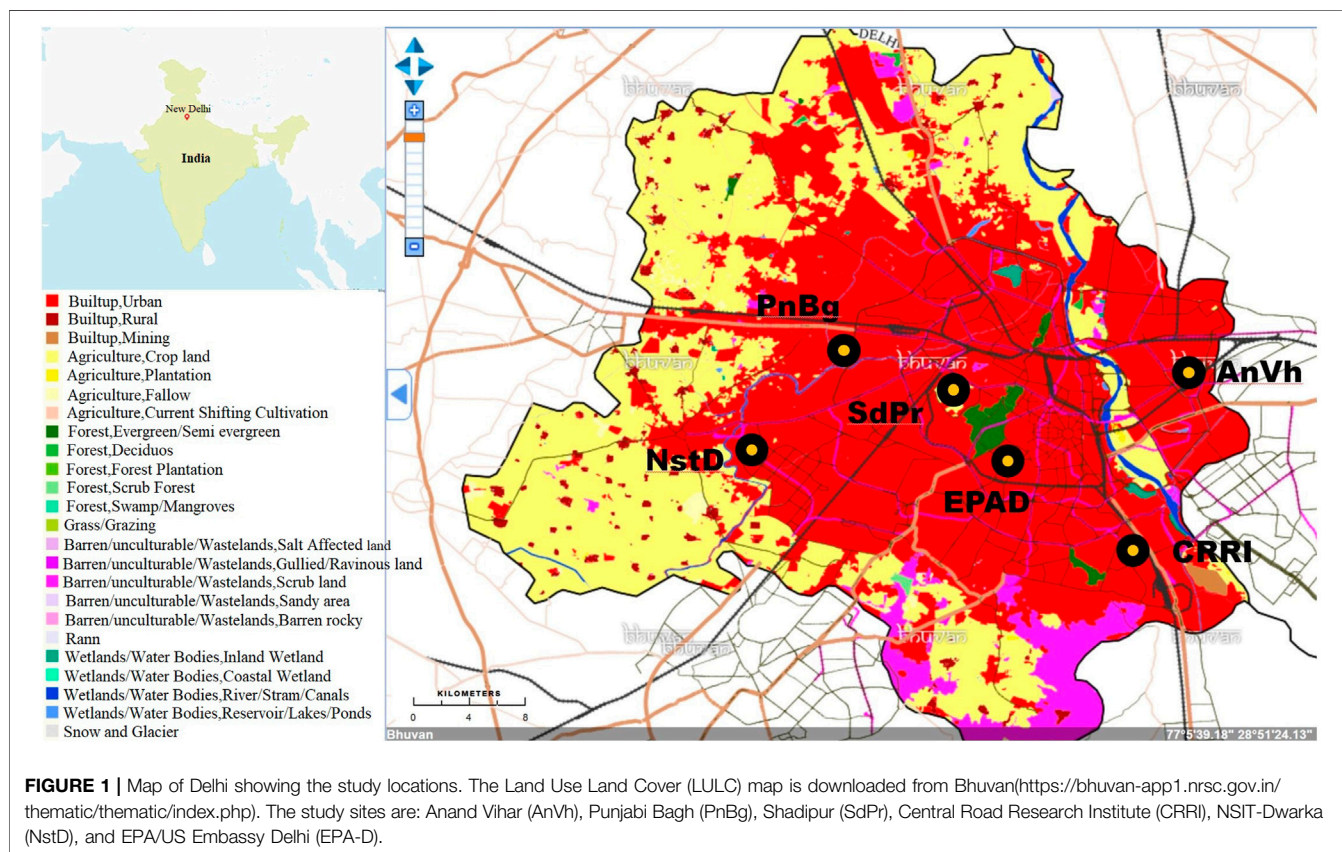
<sup>5</sup><http://delhiplanning.nic.in/sites/default/files/2%29%20Demographic%20Profile.pdf>

<sup>6</sup><http://delhiplanning.nic.in/sites/default/files/12%29%20Transport.pdf>

<sup>7</sup><https://transport.delhi.gov.in/sites/default/files/All-PDF/Total%2BVehicles%2BRegistered%2Bupto%2B31.03.2018.pdf>

**TABLE 2** | Location and characteristics of sites chosen for this study.

Station	Latitude (°N)	Longitude (°E)	Emission characteristic
Anand Vihar (AnVh)	28.65	77.30	Residential, major interstate bus terminal
Punjabi Bagh (PnBg)	28.67	77.13	Residential cum commercial
Shadipur (SdPr)	28.65	77.16	Residential cum commercial
Central Road Research Institute (CRRl)	28.55	77.27	Waste disposal, major highway with heavy traffic
NSIT-Dwarka (NstD)	28.61	77.04	Waste disposal, residential
EPA/US Embassy Delhi (EPA-D)	28.60	77.19	Office area, gardens around

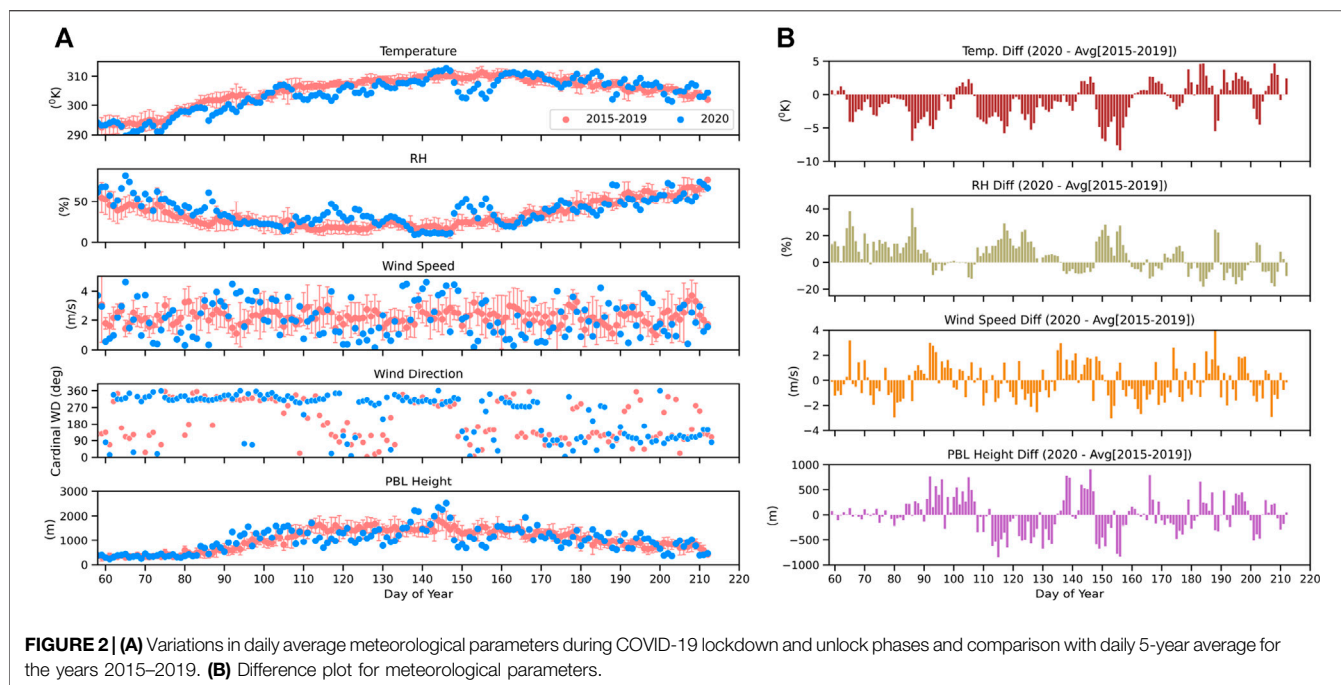


of SO<sub>2</sub>, petrol pumps (and vehicles plying) in the region can be a significant source of hydrocarbons and NO<sub>x</sub> impacting local O<sub>3</sub> chemistry.

The Central Road Research Institute is housed in a green campus in south east Delhi, just 1 km west of the Okhla Bird sanctuary on Mathura Road. Despite being in a green area, the measurements here would be significantly affected by sulfur and hydrocarbon emissions from landfill, with the Okhla Disposable Area of Delhi being in the immediate eastern neighborhood. The area also has several industries related to waste and garbage management. The area is surrounded by large educational hubs with IIT Delhi in the south-west and Jamia Millia Islamia in the north-east. There are a few hospitals toward the north, while industrial parks are located to the south.

The US Embassy is located in the very green and planned Chanakyapuri area of New Delhi surrounded by parks and

other tourist attractions. The Rashtrapati Bhavan is less than 1 km to the north, Central Ridge Reserve Forest to the west, office/market/religious areas to the south, and Safdarjung Airport to the east. The major local emissions in this area are likely to be from the transport sector, mostly light motor vehicles. Shadipur and Punjabi Bagh are located less than 2 km apart in Central West Delhi and can be characterized as residential cum commercial area. Additionally, the Naraina Industrial Area lies 1 km south of Shadipur, while the Mangolpuri Industrial Area and Ordinance Depot (Shakurbasti) lie north of Punjabi Bagh, so both these areas are likely to be impacted by mixed emission regimes. Netaji Subhas University of Technology, Dwarka (NstD, henceforth NSIT-Dwarka) is located in the western part of Delhi in the vicinity of Indira Gandhi International Airport, the later lying to the east of the monitoring station in the educational institute.



About 6 km to the north is situated the Scion Waste Water treatment plant. The Keshopur Sewage Treatment Plant is also in close vicinity.

## Meteorological Parameters

The National Centres for Environmental Prediction (NCEP) Final (NCEP FNL) operational global analysis data are produced at  $1^\circ \times 1^\circ$  grid horizontally and 26 pressure levels vertically every 6 h using Global Data Assimilation System (GDAS). The GDAS assimilates all the observations such that the model produced gridded values are consistent with observations. For all practical purposes the reanalysis data are proxy for observations. The same data-set was also used to run the FLEXPART model described later. **Figure 2** shows the 24 h average values of meteorology over New Delhi using NCEP FNL reanalysis data (National Centers for Environmental Prediction (NCEP)/National Weather Service/NOAA/U.S. Department of Commerce, 2000). The red dots show the daily 5 year (2015–2019) average of the value on a given day along with standard deviation whereas blue dots show the daily average of 2020. Five year mean values of temperatures steadily rose from March to mid-May and then started decreasing. The temperature in 2020 followed nearly the same trend as 5 year mean but in about three instances that were around day numbers 85, 110, and 150, a sudden decrease in temperature for a few days was observed. Corresponding to each of these three events, an increase in Relative Humidity (RH) and wind speed was observed. Overall, RH follows an inverse pattern of temperature variation and there is no systematic seasonal variation in wind speed. The planetary boundary layer height is low in March. It rises steadily in April and then remains high till the middle of June. Subsequently, it decreases but rather slowly.

## Source of Data Trace Gases and Particulate Matter

The Central Pollution Control Board (CPCB) monitors ambient air quality across stations spanning the entire Indian region with the help of the State Pollution Control Boards and other agencies under the National Air Quality Monitoring Programme (NAMP). Under NAMP, four air pollutants, viz.  $\text{SO}_2$ , oxides of nitrogen as  $\text{NO}_2$ , suspended particulate matter, and respirable suspended particulate matter, were identified for regular monitoring<sup>8</sup>. Along with it, measurements of  $\text{O}_3$  and CO are also available for many stations. PM measurements include  $\text{PM}_{2.5}$  and  $\text{PM}_{10}$ . The suite of instruments constitutes a Continuous Ambient Air Quality Monitoring (CAAQM) station. Currently, monitoring is carried out over 233 CAAQM stations, mostly representing urban and industrial locations. In most cases, the monitoring data is available on an hourly basis. The data can be downloaded from the CPCB portal<sup>9</sup>. A major objective of CBCB for making these measurements is to present the Air Quality Indices (AQI)<sup>10</sup>. The AQI are used for resource allocation, enforcement of standards, to determine evolution (improvement/degradation) of air quality, to raise public awareness using simple infographics, and of course to help in scientific research. For this study, CAAQM station data were downloaded for 6 sites in Delhi as described in *The Study Locations*. The parameters considered for this study are  $\text{PM}_{10}$ ,  $\text{PM}_{2.5}$ ,  $\text{NO}_2$ ,  $\text{O}_3$ , CO, and  $\text{SO}_2$ .

<sup>8</sup><http://cpcb.nic.in/air.php>

<sup>9</sup><https://app.cpcbccr.com/ccr/#/caaqm-dashboard/caaqm-landing/caaqm-comparison-data>

<sup>10</sup>[https://app.cpcbccr.com/ccr\\_docs/FINAL-REPORT\\_AQI.pdf](https://app.cpcbccr.com/ccr_docs/FINAL-REPORT_AQI.pdf)

The ultraviolet photometric O<sub>3</sub> gas analyzers work on the standard principle of absorption of radiation at 254.7 nm by atmospheric O<sub>3</sub>. The lower detection limit of the instrument is 1 ppb with a response time of 30 s or less. The CO instruments are based on gas filter correlation technology and operate on the principle of infrared absorption at 4.67 μm vibration-rotation band of CO (Nedelec et al., 2003). It has a lower detection limit of 100 ppbv at a 60 s response time. The zero noise of the instrument is 20 ppbv root-mean-square (RMS) at 30 s averaging time. The NO<sub>x</sub> instruments are based on the detection of chemiluminescence produced by the oxidation of nitric oxide (NO) by O<sub>3</sub> molecules, which peak at 630 nm radiation (Navas et al., 1997). The method is specific to NO only. NO<sub>2</sub> is measured by converting it into NO using a molybdenum convertor and then measuring total NO<sub>x</sub> as NO. Unfortunately, the reduction of NO<sub>2</sub> to NO is not specific for NO<sub>2</sub>, and other nitrogen species are also reduced to NO and act as interferences in the NO<sub>2</sub> measurements. The lower detection limits of these instruments are approximately 1 ppb at a response time of 120 s or less. The SO<sub>2</sub> measurements are based on UV fluorescence wherein SO<sub>2</sub> is excited using 214 nm and a band pass filter centered approximately 350 nm is used to collect the fluorescence (Mallik et al., 2016). The PM<sub>10</sub> measurements are based on the principle of β-ray attenuation. The particulate matter in ambient air is sampled through the instrument at a flow rate of 16 liters per minute and collected on fiberglass filter tape. Comparison of measurements of β-ray radiation by scintillation/G.M. counter before and after sampling gives a measure of the amount of PM<sub>10</sub>. The PM<sub>2.5</sub> measurements are similar to PM<sub>10</sub> but the particle size cutoff is in the range of 0–2.5 μm. The instrument specifications for obtaining these measurements can be found in the CPCB website<sup>8</sup>.

We have used daily average data for 5 selected sites from January, 2015 to July, 2020. However, there are data gaps for various species e.g. data for Central Road Research Institute are only available from the last quarter of 2017 (except availability of intermittent data in 2015: Jan–Apr, Sep–Nov), while data from Anand Vihar are missing during Jun–Oct 2017. Similarly data from Punjabi Bagh are missing from Nov 2016 to Oct 2017, while data from Shadipur is missing during Apr–Sep 2017. PM data of NSIT-Dwarka is missing during Dec 2015–Sep 2017.

### Satellite Data

Ozone Monitoring Instrument (OMI) is a spectrometer on board NASA EOS Aura satellite in sun-synchronous orbit with local equator crossing time 13:45 ± 0:15 h (Levelt et al., 2006). The spectrometer has a field of view 13 km × 24 km near nadir and 24 km × 160 km at the edges of swath. It has three channels—two in UV wavelength range and one in visible wavelength range with subnanometer spectral resolution. Columnar NO<sub>2</sub> concentrations are estimated using visible channel radiance values in wavelength range 405–465 using the algorithm described in Lamsal et al. (2020). The NO<sub>2</sub> spatial maps (0.25° × 0.25°) are made using cloud screened L3 data (Version 3) from OMI obtained through Giovanni interface<sup>11</sup>. For the rest of the

calculations and plots in this work, Version 4 OMI NO<sub>2</sub> standard product (Krotkov et al., 2019) is used. The version 4 update includes use of field of view specific geometry dependent Lambertian surface reflectivity in NO<sub>2</sub> retrieval and more accurate terrain pressure among several other improvements and has uncertainty less than 30%.

Visible Infrared Imager-Radiometer Suite (VIIRS) is a whiskbroom radiometer with 22 channels ranging from 0.41 to 12.01 μm on board Suomi National Polar-orbiting Partnership (NPP) satellite platform that was launched in October 2011. The VIIRS sensor is designed to extend and improve upon its predecessor namely MODIS and AVHRR. There are two different algorithms to estimate aerosol optical depth (AOD) (Levy et al., 2015; Sawyer et al., 2020). In this work, AOD estimated using the dark target algorithm is used (Levy et al., 2020)<sup>12</sup>.

### FLEXPART Model

FLEXPART (FLEXible PARTicle dispersion model) is an open-source Lagrangian particle dispersion model. The FLEXPART model can be run in forward or backward mode using user-supplied meteorological fields and allows for physical processes such as dry deposition, wet deposition, diffusion, convective transport, etc. to estimate dispersion or source-receptor relationships (Seibert and Frank, 2004; Pisso et al., 2019). The latest version 10.4 was run in backward mode to calculate source-receptor relationship for Delhi for each day starting from 15 January to 31 July in the current work. The source-receptor relationship is the sensitivity to the emissions located at a given grid-box for the receptor location. It represents the normalized total time spent by the back-trajectories in a given grid-box. We used 50000 trajectories spread over 24 h to estimate source receptor relationship for each day. A few source-receptor relationships for the grid-boxes close to the earth's surface are shown in Figure 7.

### Emission Sources and Lifetimes of Species Emission Sources of Various Species

The National Capital Region (NCR) covering Delhi and adjoining regions is changing with time and so are the emissions of various species. The major factors are increasing population, vehicular activities, industries, demand for power, domestic emissions, etc. There were various attempts to estimate the emissions from these sources. Guttikunda and Calori (2013) made emission inventory for particulate matter and various trace species at a resolution of 1 km × 1 km (Table 3). The major pollution sources are transportation, power generation, and construction activities. Sindhwani et al. (2015) developed emission inventory for the criteria pollutants such as PM<sub>10</sub>, NO<sub>x</sub>, SO<sub>2</sub>, and CO at 2 km × 2 km resolution for the NCR for 2010. Major emission sources of the region include vehicular exhaust, road-dust, domestic, industrial, power plants, brick kiln etc. Sahu et al. (2015) developed a high-resolution emission inventory for two major atmospheric pollutants, NO<sub>x</sub> and CO. The inventory was developed with a grid resolution of 1.67 km × 1.67 km for the

<sup>8</sup><http://cpcb.nic.in/air.php>

<sup>11</sup><https://giovanni.gsfc.nasa.gov/giovanni/>

<sup>12</sup><https://ladsweb.modaps.eosdis.nasa.gov/>

**TABLE 3** | Sector-wise source contributions (%) to particulate matter and various trace gases.

Source	PM <sub>2.5</sub>		PM <sub>10</sub>		NO <sub>x</sub>			CO			SO <sub>2</sub>		VOCs
	GC	GC	Setal	GC	Setal	SB	GC	Setal	SB	GC	Setal	GC	
Transport	17	13	19	53	47	63	18	46	60	2	14	51	
Power plant	16	15	13	7	7	3	31	-	-	55	67	13	
Industries	14	11	10	11	13	31	15	16	2	23	9	5	
Domestic	12	8	7	1	1	3	14	15	38	6	2	7	
Brick Kiln	15	11	11	2	2	-	12	12	-	11	4	9	
Construction	5	9	1	-	-	-	-	-	-	-	-	-	
Waste burning	8	7	6	1	2	-	2	3	-	2	1	-	
Diesel Gen sets	6	4	5	25	27	-	7	8	4	2	14	-	
Road dust	6	22	20	-	-	-	-	-	-	-	-	-	
Total kTons/yr	63.0	114.0	107.6	376.0	342.3	255.4	1,425.0	1,290.1	703.2	37.0	83.2	261.0	

NCR using Geographical Information System (GIS) technique for base year 2010. The emission estimates from these inventories are presented in **Table 3**.

### Lifetimes of Species

The chemical lifetime for a species, which has photochemical loss, is defined as the inverse of its total loss rate (Seinfeld and Pandis, 2006). More reactive species will have shorter lifetimes. Particles do not have fast chemical loss like gases but they settle down to various surfaces. Coarse (bigger) particles (such as PM<sub>10</sub> and bigger) have shorter lifetime, while the finer (smaller) ones (PM<sub>2.5</sub>) have longer lifetime (Textor et al., 2006; Croft et al., 2014; Kristiansen et al., 2016). Many species such as SO<sub>2</sub> and O<sub>3</sub> also have significant loss due to dry deposition. Furthermore, loss rates are higher leading to shorter lifetimes in a polluted atmosphere compared to cleaner regions. Also, chemical lifetimes are shorter in summer than in winter for species having photochemical losses. Williams et al. (2012) have estimated aerosol lifetime as a function of particle size and as a function of altitude using data gathered during Indian Ocean Experiment. They found a lifetime of approximately 1.5 days for aerosols in the boundary layer for particle sizes between 0.08 and 0.1 μm. Larger size particles known as super micron size particles (1.1–10 μm) have shorter residence time. Grythe et al. (2017) found a lifetime of particles greater than 1 μm radius to be less than a day.

O<sub>3</sub> has a short lifetime, typically hours, in polluted urban regions where concentrations of its precursors are high (Stevenson et al., 2006; Conley et al., 2012; Young et al., 2013; Monks et al., 2015). Based on the estimated values of hydroxyl radical (OH) over the northern Indian Ocean, which were several times higher than the global average OH concentration of approximately  $1 \times 10^6$  molecules cm<sup>-3</sup>, Lawrence and Lelieveld (2010) found lifetime of CO of only ~15 days near the surface, and a NO<sub>x</sub> lifetime of less than a day.

The atmospheric lifetime of NO<sub>x</sub> depends on various processes occurring in the atmosphere including the photolysis of NO<sub>2</sub> and the hydroxyl-mediated oxidation of NO<sub>2</sub>; thus, its lifetime depends on the concentration of other constituents (Levy et al., 1999; Shah et al., 2020). Liu et al. (2016) estimated the NO<sub>x</sub> lifetime using OMI satellite data and ECMWF wind fields over polluted cities and power plants in polluted background and have found it to be  $3.8 \pm 1.0$  h. The lifetime of SO<sub>2</sub> is approximately 1.8 days within the boundary layer depending upon the

meteorological conditions and the removal by OH-induced gas-phase conversion into gaseous sulphuric acid (Inomata et al., 2006; Lee et al., 2008).

## RESULTS AND DISCUSSIONS

### Satellite Observations

**Figure 3** shows a pictorial representation of COVID-19 effect on anthropogenic air pollution represented by tropospheric column NO<sub>2</sub> (Tropo col NO<sub>2</sub>) changes during COVID-19 months (2020) over the Indian region w.r.t. similar period in the previous year (2019). Most of the boundary layer NO<sub>2</sub> can be specifically attributed to its anthropogenic sources, which were the most impacted as a result of lockdown. The effect is clearly visible in much reduced tropospheric column NO<sub>2</sub> concentrations during COVID-19 months.

**Figure 4** shows monthly average columnar concentration of tropospheric col NO<sub>2</sub> over a latitude longitude range of 28.465°N–28.715°N and 77.065°E–77.315°E that covers the NCR around New Delhi. The vertical bars are  $\pm 1$  sigma standard deviations. A clear decrease of tropospheric column NO<sub>2</sub> amount can be seen in the months of April (–45%), May (–42%), and June (–26%). March 2020 does not show a clear decrease because the lockdown was implemented only in the last week of March (**Table 1**). The decrease in NO<sub>2</sub> ceases to be significant in July (–6%) as lockdown measures were restricted to few containment zones (**Table 1**).

**Figure 5** shows monthly average of aerosol optical depth (AOD) over New Delhi. Despite a large year to year and monthly variability, a significant decrease in AOD is observed. Usually an increase in AOD values is observed over Delhi from March to June (Pandithurai et al., 2008) but in 2020, AOD values were low during the lockdown period starting from April to June compared to the same month in previous years. We believe this was because of reduced anthropogenic emissions during the lockdown. A major source of aerosols in Delhi during summer has been found to be fugitive dust particles from roads, and the construction sector accentuated by windblown dust. A receptor-based modeling approach by ARAI and TERI estimated influence of nearly 42% to PM<sub>10</sub> and 34% to PM<sub>2.5</sub> from this sector for the summer months (ARAI and TERI, 2018). The road transport and the construction works were severely limited during the

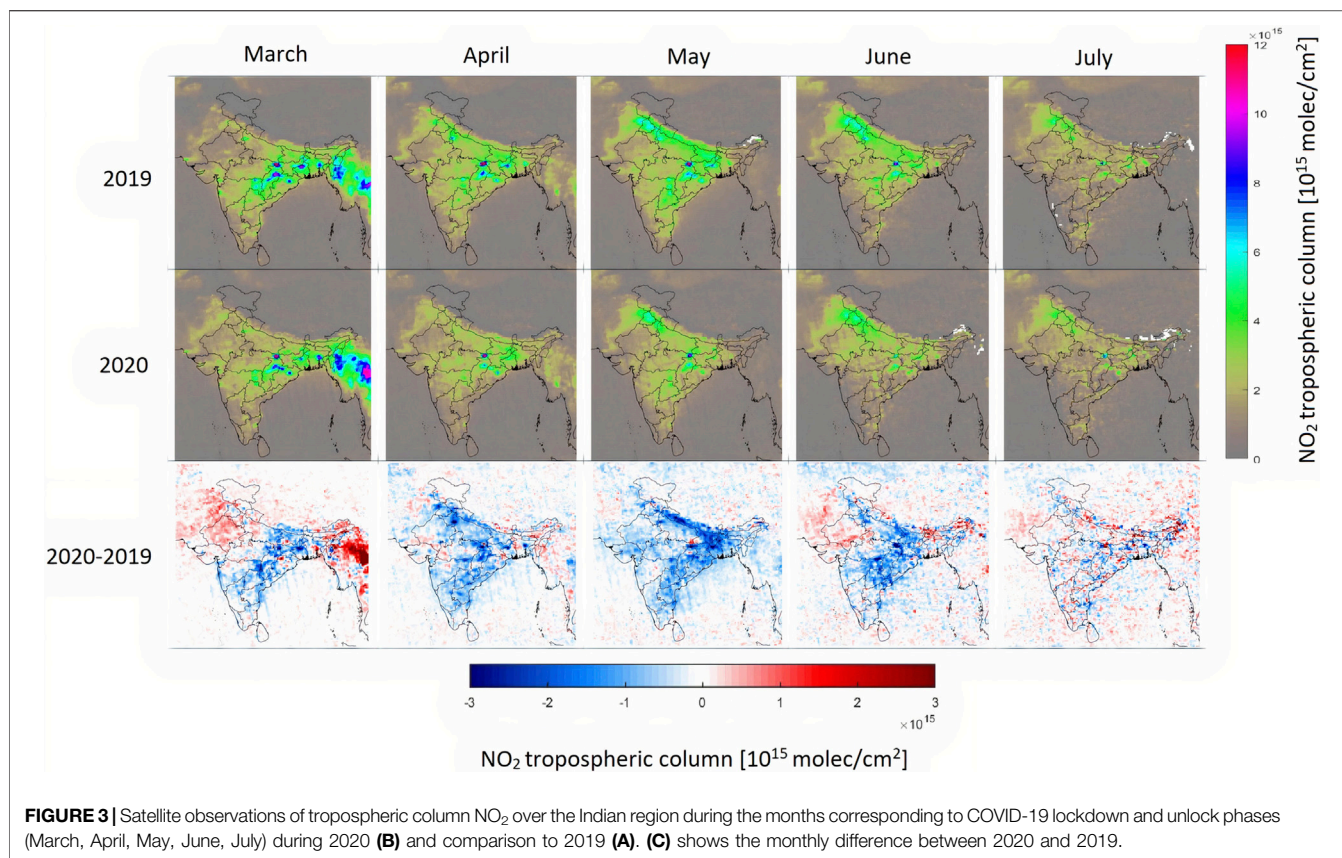


**FIGURE 3** | Satellite observations of tropospheric column NO<sub>2</sub> over the Indian region during the months corresponding to COVID-19 lockdown and unlock phases (March, April, May, June, July) during 2020 (B) and comparison to 2019 (A). (C) shows the monthly difference between 2020 and 2019.

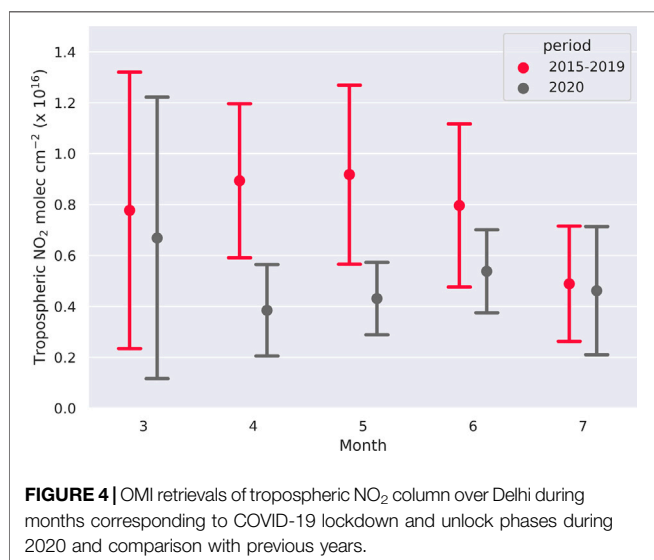


**FIGURE 4** | OMI retrievals of tropospheric NO<sub>2</sub> column over Delhi during months corresponding to COVID-19 lockdown and unlock phases during 2020 and comparison with previous years.

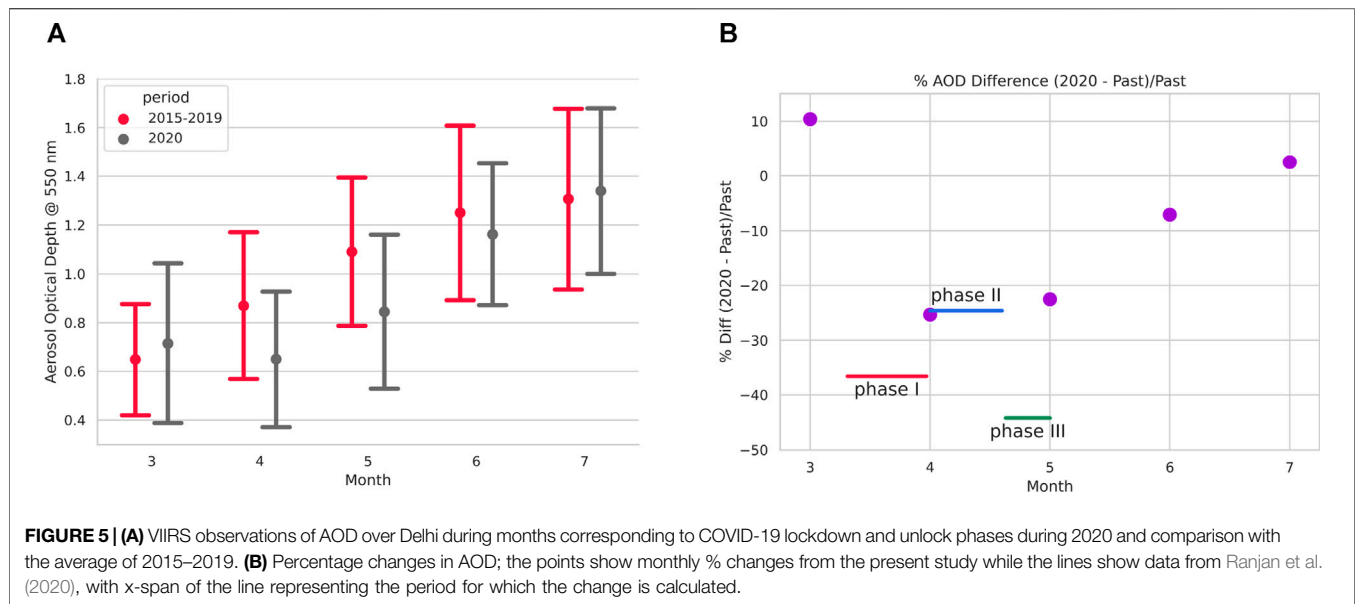
lockdown period, due to both Government mandate and exodus of migrant workers from Delhi. As a result, the natural increase in AOD was balanced by a decrease from the anthropogenic sector, cumulating into a scenario where AOD remained peculiarly flat during the summer months with lower values during 2020 year compared to previous years (2015–2019) and a decrease in monthly values until June is observed. A recent study revealed

that AOD decrease over India during lockdown was of the order of 45%, while the AOD anomaly over Delhi NCR was  $-24.6\%$  during the 2nd half of April and  $-44.2\%$  during the first half of May (Ranjan et al., 2020). Furthermore, we observe an enhancement of AOD during March (10.4%) but reductions of 25.3 and 22.5% in April and May respectively when calculating the anomaly against 2015–2019. In June, the AOD values were only 7% lower than the 5 year mean and in July, the AOD values for 2020 were 2.4% higher than 5 year mean. The difference between our estimates and Ranjan et al.'s (2020) estimates is because of the fact that Ranjan et al. have used average from 2000 to 2019 whereas we have used average of 2015–2019 for the comparison (Figure 5B). Another reason could be the resolution of the data used; we have used  $0.5 \times 0.5$  degree area while Ranjan et al. have used very high spatial resolution (1 km) data.

## Ground-Based Observations

The above explanations for AOD and NO<sub>2</sub> represent an integrated atmospheric change as a result of COVID-19 lockdown. However, most of the emission changes occur close to the surface. Therefore, we present a detailed analysis of surface observations.

To understand the changes in atmospheric concentrations of trace gases and particulate matter as a result of changed emission scenarios, the daily variation of these parameters during March–July, 2020 is compared with the average of 2015–2019 of the same period and for the same parameters. An example plot

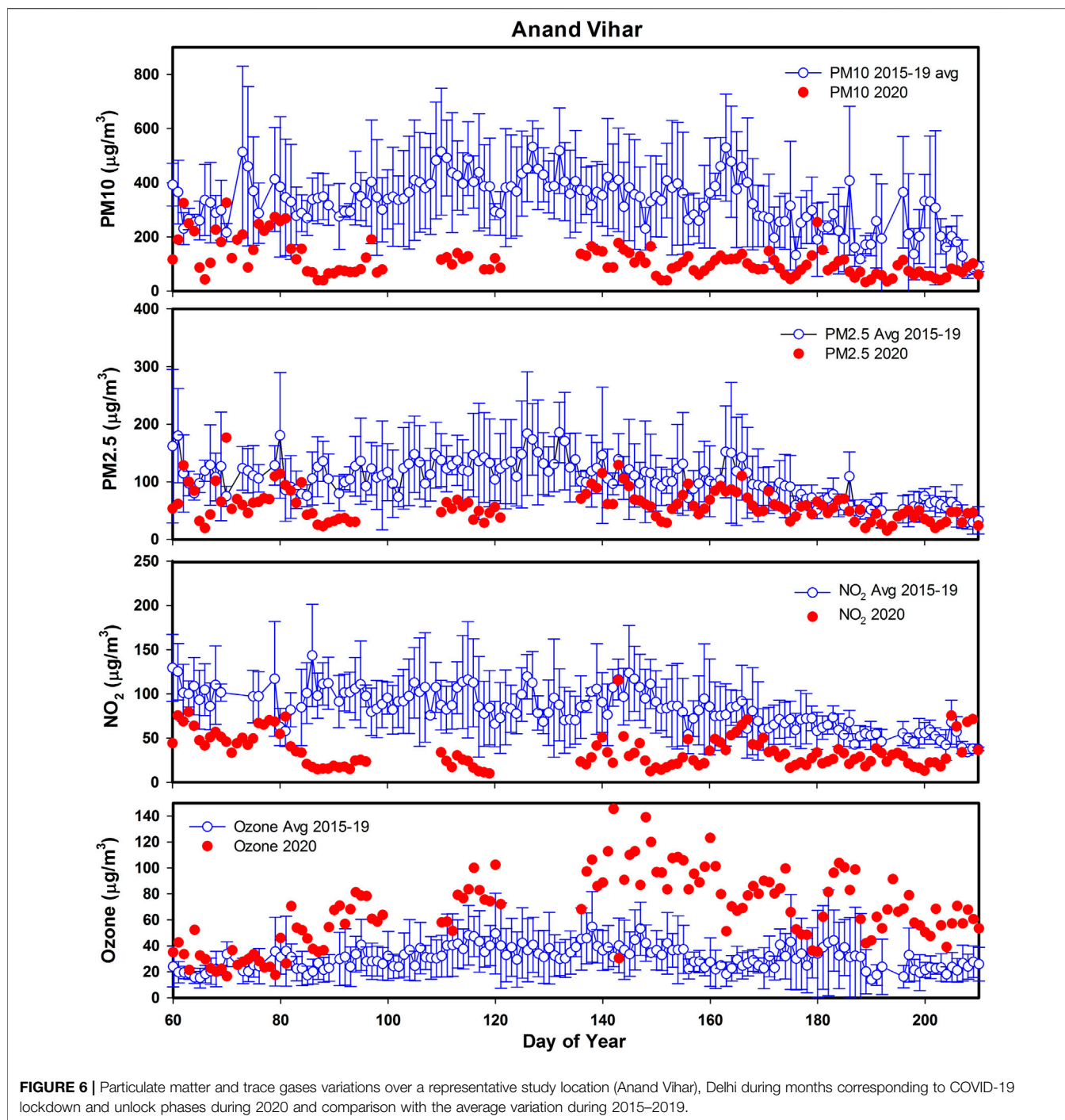


for Anand Vihar is shown in **Figure 6**. It is observed that the two datasets start to diverge around day of year (DOY) -85, representing 25 March, the day of initiation of nationwide lockdown (**Table 1**). The divergence around this period is maximum for  $\text{NO}_2$  followed by  $\text{PM}_{10}$  and  $\text{PM}_{2.5}$ . The divergence is also significant in  $\text{O}_3$ . This indicates that the sources impacted by lockdown play a crucial role in the budgets of  $\text{NO}_2$  and PM (2.5 and 10). The patterns for PM and  $\text{NO}_2$  are more or less similar for different stations but this does not hold so for  $\text{O}_3$ . This is on expected lines as the major sources of PM e.g., transport sector and road dust account for 30–40% of  $\text{PM}_{10}$  over Delhi. Similarly, transport sector makes a major contribution in the anthropogenic  $\text{NO}_2$  sources. As a result, the departure in  $\text{NO}_2$  is drastic both in satellite-based columnar data and at surface level (**Figures 4, 6**). However, not much change is observed for CO, as major sources of CO are related to combustion i.e., biofuels and biomass burning which were not directly affected by lockdown processes. However,  $\text{O}_3$  presents a different picture as its concentration is a complex interplay of atmospheric transport processes, changes in primary emissions, meteorology and photochemistry in addition to chemical and depositional losses. These changes in surface level pollutants are further discussed below.

## Aerosols

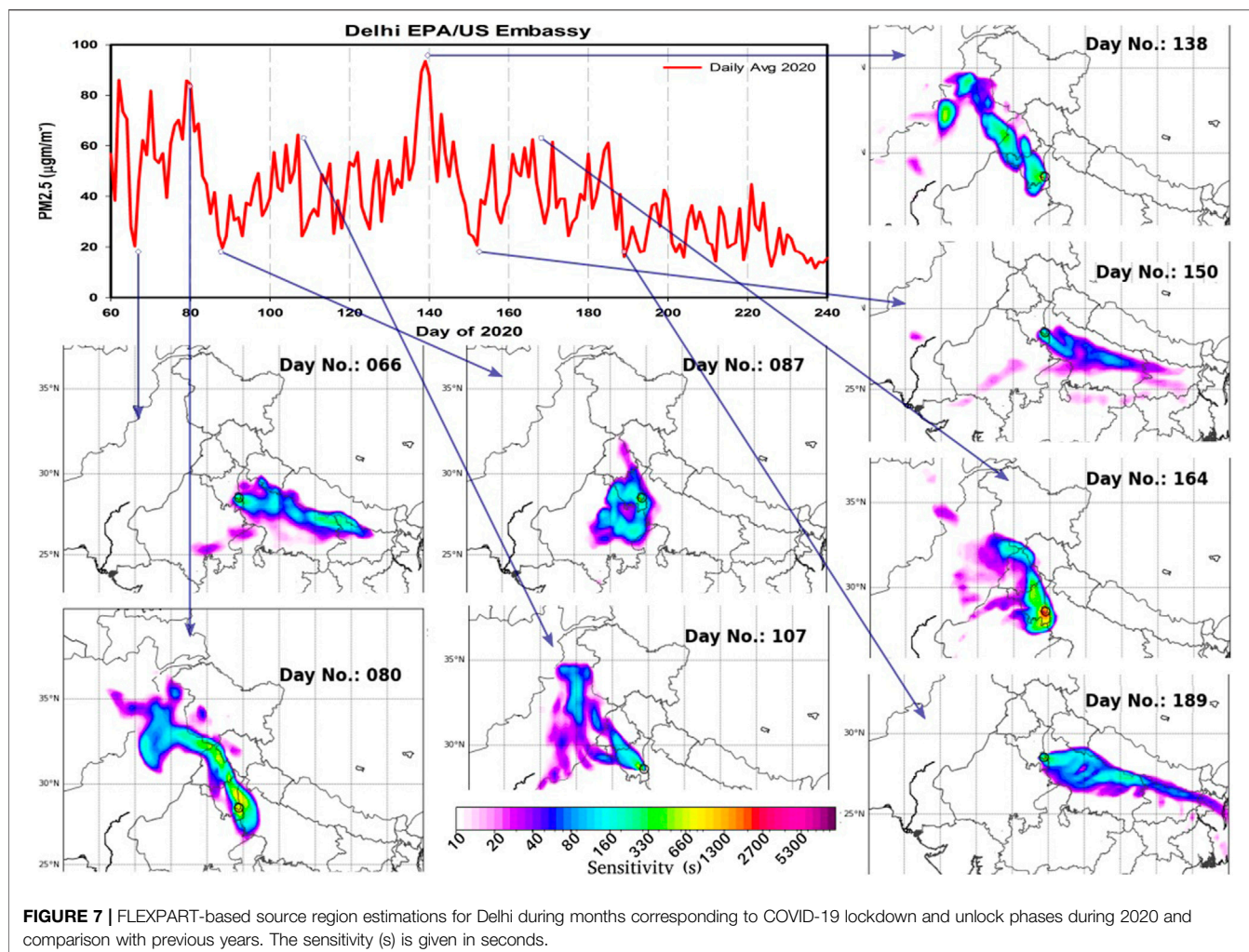
High amounts of atmospheric aerosols negatively affect health and air quality, and hence constitute criteria pollutant for the measure of air quality. Indian cities in general suffer from poor air quality mostly due to aerosols (SOGA, 2020). India's capital city, Delhi, is particularly badly affected by air pollution. In a particularly grave event,  $\text{PM}_{2.5}$  concentrations (peak 24 h average  $650 \mu\text{g m}^{-3}$ ) exceeded the Indian air quality standards by 11 times and the World Health Organisation (WHO) guidelines by 25 times in early November 2017. Beig et al. (2019) studied this event and found that combined effect of a dust storm in the middle-east, agricultural waste burning in

upwind states, and stagnation of local air pollution led to this event. The mortality rate due to pollution in Delhi is estimated to be very high and the city is projected to be among the top 5 cities in the world to have high fatality rates (Apte et al., 2015; Lelieveld et al., 2015). Air pollution caused between 10000 and 30000 premature deaths in Delhi in 2015 (Bithal, 2018). While air pollution is particularly bad in winter over Delhi, the  $\text{PM}_{2.5}$  levels are often higher than the WHO limit of  $25 \mu\text{g m}^{-3}$  and the Indian Air Quality Standard of  $60 \mu\text{g m}^{-3}$  for most part of year except during the rainy months of July and August (Bali et al., 2019; Hama et al., 2020). Main sources of  $\text{PM}_{2.5}$  particles are anthropogenic emissions except when there is a dust storm like event. In a past study, chemical make-up of  $\text{PM}_{10}$  aerosol over Delhi was found to be 20% organic, 6% combustion, 31% secondary inorganic, and 43% soil particles during the spring season. While for the most part of India, the residential sector is a major emitter of  $\text{PM}_{2.5}$  particles, over Delhi it is the transport sector with nearly 64% contribution (Conibear et al., 2018; Reddington et al., 2019). Beig et al. (2019) attributed 65% of observed  $\text{PM}_{2.5}$  concentration to dust and smoke transport from upwind regions for a high pollution event during November 2017. However, this fractionation may not be applicable for all seasons and local emissions may have far more dominating influence on the total concentration. This is because overall wind direction and boundary layer characteristics are different in summer and winter as one can see from the FLEXPART output (**Figure 7**), as well as the meteorological plots shown in **Figure 2**. While winter time air pollution over Delhi is studied more frequently because of very high aerosol concentration making them visible and perceptible as a health threat in public mind, concentrations in summer, even though lower than the winter months, are still high enough to pose serious health hazards when exposed for a long time but they are less frequently studied. A campaign-based study during January–March, 2018 over multiple sites in Delhi region using three aerosol mass spectrometers (AMS) for non-refractory fraction, two aethalometers, and one single particle soot



photometer concluded that local pollution was dominating over regional pollution during this period (Lalchandani et al., 2021). This was based on the observation of similar chemical composition both within Delhi-NCR and downwind region with mean  $\text{PM}_{2.5}$  reaching  $153.8 \pm 109.4 \mu\text{g m}^{-3}$  with major contribution from organics (43–47%) followed by chloride (11–17%), ammonium (9–13%), sulfate (8–13%), nitrate (9–11%), and (5–16%) black carbon. However, significant fraction of highly oxidized, low volatile organic aerosols to the

oxygenated organic aerosol (OOA) fraction indicated influence of regional transport, which was attributed to the north-west direction of the study sites. A detailed chemical characterization of  $\text{PM}_{2.5}$  over Delhi for heavy and trace elements using the Energy Dispersive X-ray Fluorescence technique during post-monsoon of 2019 concluded large influence from agriculture-residue burning emissions in north-west Indo-Gangetic Plains (IGP) (Bangar et al., 2021). In contrast to winter pattern, during warm season, Jain et al. (2020) observed



higher amount of secondary sulphate over secondary nitrate indicating higher contribution from point sources. A higher contribution of secondary organic carbon during pre-monsoon compared to post-monsoon was found over Delhi during a study employing stable carbon isotope analysis (Singh et al., 2021). The study confirmed the dominance of C3 plant-derived aerosols over Delhi, which could be sourced from agriculture residue burning transported from outside the city. Air mass trajectory cluster analysis using HYSPLIT over Delhi during January 2013–June 2014 indicates that the air mass approaches from 4 sides [north-western IGP, Pakistan (10%); north-western IGP, north-west Asia (45%); eastern IGP (38%); Pakistan and Arabian Sea (6%)] (Sharma et al., 2016). The authors concluded that  $PM_{10}$  over Delhi is dominated by soil dust (22.7%) followed by secondary aerosols (20.5%), vehicle emissions (17.0%), fossil fuel burning (15.5%), biomass burning (12.2%), industrial emissions (7.3%), and sea salts (4.8%). The lockdown provided a unique opportunity to study causes of air pollution and evaluate sectoral contributions during the summer months.

**Figure 7** shows the source-receptor matrix calculated using FLEXPART for select days when  $PM_{2.5}$  concentrations were observed high or low. The air masses were from the north-

west direction during initial phases of lockdown (March), but during later phases after the onset of monsoon over Delhi in June, the air masses became easterly over Delhi, bringing in pollutants from the eastern IGP. Interestingly, in **Figure 7**, higher peaks in  $PM_{2.5}$  coincide with north-westerly air-masses sourced to industrial regions in Haryana and Punjab of India all the way back to Lahore in Pakistan and further back to the north-west. Lalchandani et al. (2021) have shown through high-precision AMS measurements that air mass transport from north-west air over different sites in Delhi is associated with conspicuous amount of highly volatile and semi-volatile OOA. Higher levels of tropospheric  $NO_2$  column values can be seen in the month of May (**Figure 3**) toward the north-west of Delhi and up to Pakistan in the IGP which suggests heavy pollution due to industrialization in this area. The high patch of  $NO_2$  column gets diluted in June as the influence of monsoon winds starts. Lower values of  $PM_{2.5}$  are related to the atmospheric transport either circulating around NCR or coming from the eastern part of IGP, where  $NO_2$  columns already evince relatively lower values. Hence, major changes in  $PM_{2.5}$  are likely associated with the transport from the corresponding  $NO_2$  column regions.

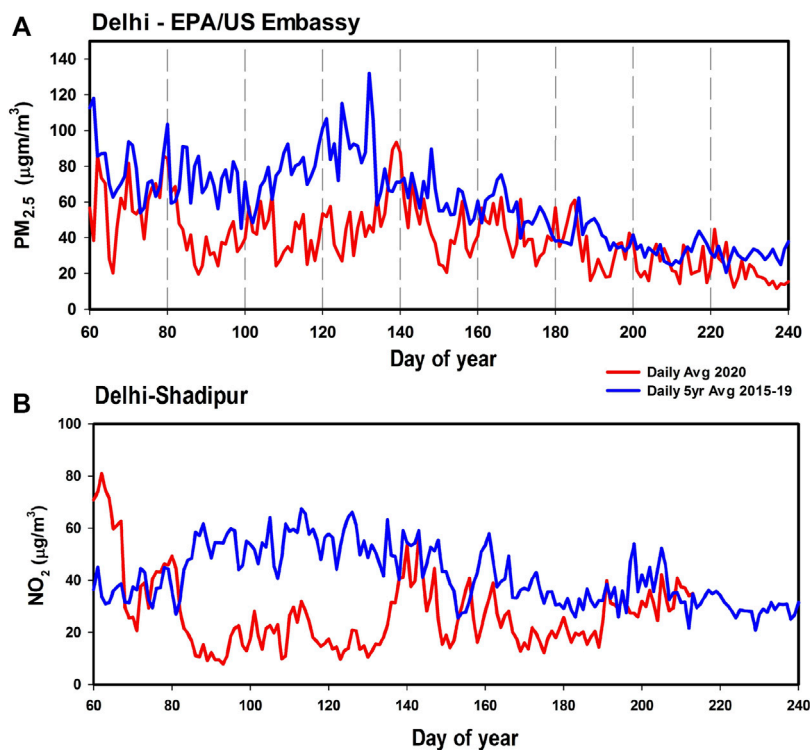


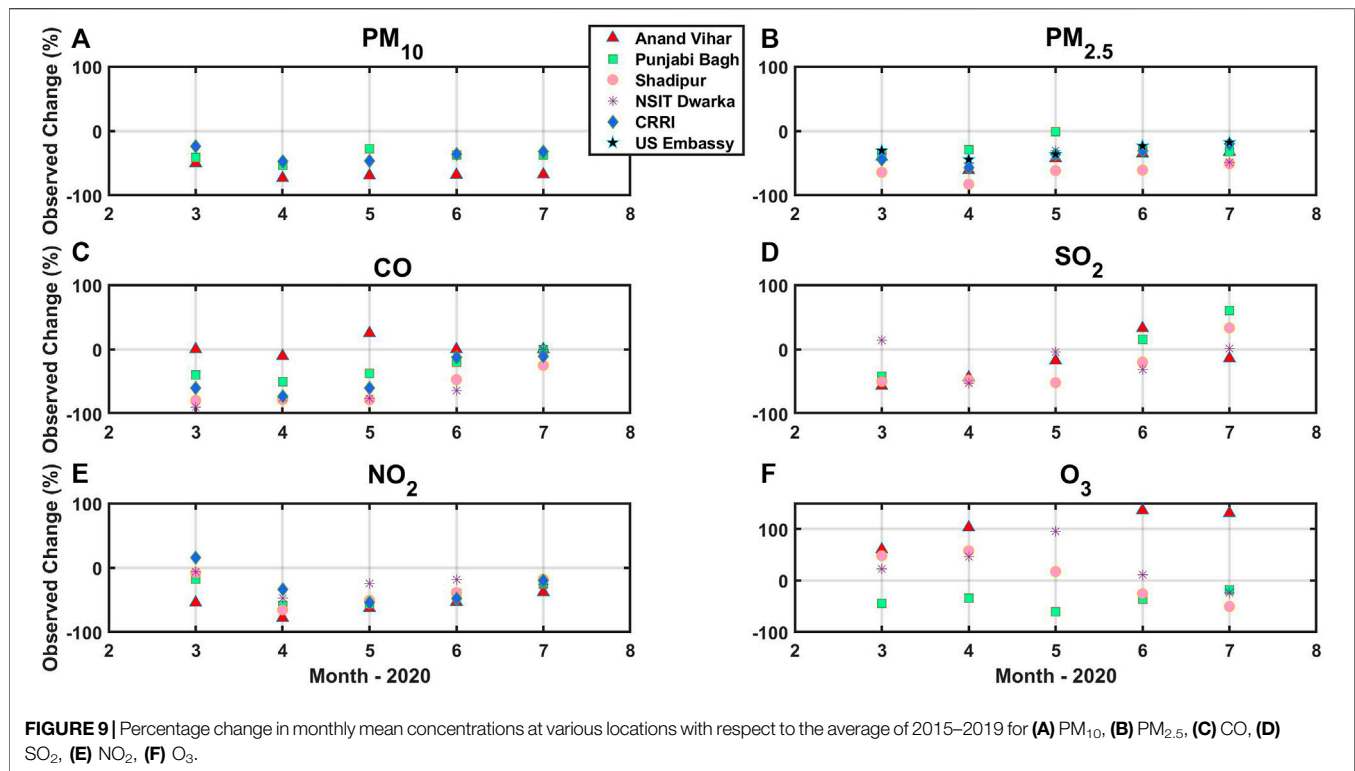
**FIGURE 8 | (A)** PM<sub>2.5</sub> variation observed at US Embassy New Delhi during the COVID period from 1 March to 31 July (red curve). It is compared with 5 year period (2015–2019) (blue line). **(B)** Similar to PM<sub>2.5</sub> but for NO<sub>2</sub> observed at Shadipur, a location near the US Embassy site.

The PM<sub>10</sub> concentration, which is found to be in the range of 80–270 µg m<sup>-3</sup> in IGP in the previous years, was reduced to ~70 µg m<sup>-3</sup> during the lockdown. Daily average variations of PM<sub>2.5</sub> and surface level NO<sub>2</sub> over two nearby study sites in Delhi during the lockdown period are shown in **Figures 8A,B** against the daily 5 year average of 2015–2019. As mentioned earlier, there is large variability in the 5 year average as well as during the 2020 due to transport of pollutants from the surrounding regions. While there is a general decreasing pattern from May to August because of the change in wind direction, a significant decrease in PM<sub>2.5</sub> is seen for the lock-down period despite that. Since lifetime of PM<sub>2.5</sub> is only 1–2 days (**Table 4**), sharp decrease in the levels of PM<sub>2.5</sub> was observed from the inception of the lockdown on 25th March (day #85) till at least May end (day #152). The rapid decrease also suggests that anthropogenic emissions are the significant sources of PM<sub>2.5</sub> particles over Delhi. Of course, there are two events of high PM<sub>2.5</sub>, the first from day #90 to day #105 and the second peak around day #140. Similar changes are observed even in NO<sub>2</sub> at a nearby location for example at Shadipur as shown in **Figure 8B**. This shows that these major changes are not local but in a large area covering the NCR and are due to transport from different regions as discussed above using the FLEXPART trajectories. The region in north-west of Delhi seems to contain very large sources of particulate pollution, as whenever the source region is north-west of Delhi, PM<sub>2.5</sub> concentrations are high. Aethelometer black carbon measurements over Delhi showed increased local contributions

**TABLE 4 |** Lifetimes of particulate matter (PM) and various gaseous species.

Species	Lifetime	References
PM <sub>10</sub>	Minutes to days	Seinfeld and Pandis (2006) Grythe et al. (2017)
PM <sub>2.5</sub>	1–2 days	Williams et al. (2012)
NO <sub>2</sub>	~1 day to ~ few hrs	Lawrence and Lelieveld (2010) Liu et al. (2016)
Ozone	Hours	Monks et al. (2015)
CO	15 days	Lawrence and Lelieveld (2010)
SO <sub>2</sub>	~1.8 days	Lee et al. (2008)

(fossil fuel fraction) with the progress from lockdown to unlock phase, but the fossil fuel contribution specifically dipped during 4–17 May due to intensive crop residue burning in neighboring states (Goel et al., 2021). Gadhavi et al. (2015) who analyzed black carbon concentration over a rural location in South India, also found high concentrations of black carbon particles for the days when the source region extended to north-west of Delhi compared to other days. While looking at the PM<sub>2.5</sub> concentration maps available in the literature (Bali et al., 2019; Reddington et al., 2019), one can see whole of IGP region filled with high amount of particles. The temporal variation of PM concentration when looked in connotation with FLEXPART trajectories, east of Delhi region seems to contribute much smaller amount of air pollution compared to when wind is blowing from west.



Figures 9A,B show monthly average percentage changes in 2020 with respect to the 5 year average of 2015–2019,  $[(X_{2020} - X_{2015-2019}) / X_{2015-2019}] \times 100$ , in PM<sub>10</sub> and PM<sub>2.5</sub> respectively. Unfortunately, PM<sub>10</sub> data are available only for the 3 stations from the selected locations for this work (Figure 9A). Anand Vihar shows the largest decrease in PM<sub>10</sub> as compared with the other two locations, while the other two locations show almost similar changes. Highest decrease of about 73% is observed in April, which was the month of very strict lockdown with almost all transport and industries closed. As the lockdown starts easing during each month, levels of PM<sub>10</sub> continue to increase. However, even in July the decrease is significant, smallest approximately 33% for Central Road Research Institute. This could be due to continuation of lockdown for certain activities such as educational institutes, metro services, cinema halls, restricted attendance at offices, limited domestic air travel etc., as listed in Table 1. The major sources of PM<sub>10</sub> are transport, industries, brick kiln, and dust from roads and construction activities (Table 4). All these remained closed during the lockdown and slowly and progressively allowed to return to normal. Since the lifetime of PM<sub>10</sub> is very short, only a few hours (Table 3), it shows almost an instant effect of the changes. The ratio of decreases between Punjabi Bagh and Central Road Research Institute during different months shows an average value of 1.1, which indicates a uniform impact of lockdown on PM<sub>10</sub> from north-west to south-east of urban Delhi (Figure 1). If these ratios are computed with respect to Anand Vihar to the other sites, the value is much higher, revealing that the magnitude of lockdown effect has been larger over this site with respect to PM<sub>10</sub>. As

mentioned in *The Study Locations*, Anand Vihar is located to the East of River Yamuna, comparatively more congested and impacted by mixed emissions from industries and transport sector. Furthermore, the magnitude of decreases evinces an overwhelming anthropogenic control of PM<sub>10</sub> over Delhi.

Changes in the monthly average levels of PM<sub>2.5</sub> are shown for all the five locations selected for this work (Figure 9B) and additionally include the EPA data for the US Embassy in Delhi. In general and as for PM<sub>10</sub> and also for other species, maximum decrease is observed in April. There is large variability from location to location. Shadipur shows the highest decrease of approximately 83% with respect to the 5 year average followed by Anand Vihar (approximately 61%) and other locations. Again, even in July the levels of PM<sub>2.5</sub> have not become normal, with the smallest decrease approximately 18% for the US Embassy. The emission sources of PM<sub>2.5</sub> are almost similar to that of PM<sub>10</sub> but there is a significant contribution of secondary aerosols to PM<sub>2.5</sub>. Some studies show almost 50% contribution from secondary aerosols to PM<sub>2.5</sub> mass of which nearly 30% is from secondary organic aerosol (Perrino et al., 2011; Rastogi et al., 2014). The formation of secondary aerosols is initiated by various gaseous pollutants such as NO<sub>x</sub>, SO<sub>2</sub> as well as hydrocarbon oxidation. Hence, changes in these precursors also get reflected in the levels of PM<sub>2.5</sub>. Another source apportionment study estimated daily PM<sub>2.5</sub> emissions over Delhi to be 58.7 ton/day, contributed by road dust (38%), vehicles (20%), domestic fuel burning (12%), industrial point sources (11%), concrete batching plant (6%), hotels/restaurants (3%), and municipal solid waste (MSW) burning (3%) (Nagar et al., 2017). Furthermore, the contribution from coal/fly-ash to PM<sub>2.5</sub> increased from 4.8%

in winter to 26% in summer, while the contribution from secondary inorganic aerosol decreased from 30% in winter to 15% in summer (Nagar et al., 2017). While  $PM_{10}$  decrease was highest for the Anand Vihar site (east Delhi), the  $PM_{2.5}$  decrease was highest over Central Delhi for Shadipur. The ratios of Shadipur to Anand Vihar are 1.6, 1.4, 1.5, 1.7, and 1.6, respectively, for March–July months, with an average of 1.5. This near constant ratio evinces a 50% higher impact to  $PM_{2.5}$  in Central Delhi compared to Eastern Delhi due to lockdown. Possibly, the chances of SOA formation locally can be accentuated by local emissions of precursor gases such as  $SO_2$ ,  $NO_2$  and hydrocarbons at Shadipur from industry, transport, and tourism sectors, as new construction activities as well as road dust are very limited over this region. Chemical characterization studies during summer over Delhi have found a higher contribution of  $SO_4^{2-}$ ,  $NO_3^-$ , and  $NH_4^+$  to  $PM_{2.5}$  compared to  $PM_{10}$  (ARAI and TERI, 2018). Source apportionment studies point to potential chloride sources northwest of the Indian Institute of Technology (IIT) Delhi, such as industries of salt and metal processing and thermal power plants to fine PM (Jaiprakash et al., 2017).

## Carbon Monoxide and Sulfur Dioxide

Both these species are considered primary pollutants.  $SO_2$  contributes to respiratory symptoms. High levels of CO can reduce the amount of oxygen that can be transported in the bloodstream to critical organs such as the heart and the brain resulting in dizziness, confusion, unconsciousness, and even death. Both these species are not very reactive.  $SO_2$  is formed during the burning of sulphur containing fuels, such as coal and oil, while CO is formed during the incomplete combustions e.g., fuels such as petrol, coal, or wood. In an urban environment, major sources of CO are transport, domestic cooking, brick kiln, industries, and power plants; while those of  $SO_2$  are coal burning in power plants and industries, transport sector, and diesel-generating sets (Table 3). Lifetime of CO is approximately 15 days in a polluted region, while the main sink of  $SO_2$  is deposition and has a lifetime of approximately 2 days (Table 4). Data for these two species are available for all the considered locations except for Central Road Research Institute, where  $SO_2$  is not available. However, there seem to be large variations.

Figure 9C shows the observed monthly CO changes during 2020 with respect to the 5 year average of 2015–2019. CO shows large decrease in March for Punjabi Bagh, Shadipur, Central Road Research Institute, and NSIT-Dwarka. However, the change is negligible over Anand Vihar in East Delhi. While the decrease continues over Punjabi Bagh and Central Road Research Institute in April, over NSIT-Dwarka there is a negligible increase. The May values show a decrease in Punjabi Bagh, Shadipur, and Central Road Research Institute, while an increase is observed over Anand Vihar and NSIT-Dwarka. The maximum decrease in CO is observed for Central Road Research Institute (approximately 57, 71, 63% in March, April, and May) followed by Punjabi Bagh. Although biogenic emissions constitute a major source of CO, large changes in CO similar to other anthropogenic markers e.g.,  $SO_2$  indicate overwhelming

anthropogenic components in Delhi. In a comprehensive study of air quality in 15 major cities of India using remotely sensed data, surface concentration measurements of CPCB, and Air Quality Zonal Modelling, more than 40% decrease was observed for CO in north Indian cities but for Delhi, an increase of 36% was observed (Rahaman et al., 2021). The study used data covering 43 days before and after lockdown; however, MEERA-2 observations by the same study showed a negligible decrease of 2.52%. The data for Rahaman et al. (2021) are taken from the ITO site at Delhi, which is approximately 7 km from Anand Vihar site, which shows a negligible decrease in CO unlike other sites in our study. On an average, CO decreases by over 50% during March–May, but there is large variability between individual sites e.g., negligible decrease in Anand Vihar to over 90% decrease in NSIT-Dwarka. Based on the data from the 134 observation sites of CPCB, Singh et al. (2020) concluded a decrease of CO over most parts of India. However, for the north-west region, the interquartile range for CO varied from +10% to –40% (Singh et al., 2020).

Large changes in  $SO_2$  are observed in the lockdown months of March–May in the order of 35–50% in line with  $NO_2$  and PM (Figure 9D). As the major sources of  $SO_2$  are large point sources such as power plants, under influence of a given air mass, they are likely to have a similar impact over a larger region. This is evinced by very close values of percent changes during the lockdown months. However, unlike other sites, NSIT-Dwarka did not show a decrease in  $SO_2$  during March 2020 (Figure 9D). A closer look at the site data revealed that the overall  $SO_2$  levels had been higher in the first quarter of 2020 compared to similar periods in other years. This can be attributed to increasing construction activities in this western edge of urban Delhi including sewage treatment plants. Painting activities at construction sites are also a source of  $SO_2$ . A good marker of  $SO_2$  source types is the  $SO_2$  to  $NO_2$  ratios. Renuka et al. (2020) have used it to show seasonal variation of sources at a rural site in South India. High  $SO_2$  to  $NO_2$  ratio indicates predominant impact of point sources such as power plants, while lower values indicate vehicular emissions that are rich in  $NO_x$  compared to  $SO_2$  (Mallik et al., 2015). An increase in this ratio during the initial lockdown phases indicates that the impact of vehicular emissions decreased (reduced denominator in the form of  $NO_2$ ) in comparison with point sources. The increase is particularly very clear over Anand Vihar (figure not shown). The impact of air mass change is also very evident in these ratios e.g., the values were higher over NSIT-Dwarka before onset of pre-monsoon winds indicating larger influence of point sources, while there is a sudden decrease in this ratio since mid of March. After this, as an effect of lockdown, the ratio starts to increase like other sites. Rahaman et al. (2021) have observed approximately 25% decrease in  $SO_2$  based on ITO CPCB data while an increase of 23% was observed in a nearby site (Ghaziabad, 30 km east of ITO). Satellite observations over Delhi also showed approximately 40% decrease in the Rahman et al. study. In Singh et al. (2020) study, the variation of  $SO_2$  is similar to CO with interquartile range for north-west India between +8% and –38%. Various estimates for  $SO_2$  are calculated for Delhi e.g., 9% decrease (Chhikara and Kumar, 2020), 19% decrease (Kumari

and Toshniwal, 2020), 23% decrease (Singh et al., 2020), the differences may be attributed to the different periods of estimations, but overall all studies show a decrease.

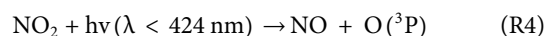
## NO<sub>2</sub>

Oxides of nitrogen such as NO and NO<sub>2</sub>, together called NO<sub>x</sub>, are important pollutants emitted from combustion at high temperature. While emissions of NO<sub>x</sub> are mostly in the form of NO, it is later converted into NO<sub>2</sub> by the reaction of NO with O<sub>3</sub>, HO<sub>2</sub>, RO<sub>2</sub>, and other oxidants. During daytime conditions of sufficient O<sub>3</sub> and radiation, NO and NO<sub>2</sub> are in a fast photochemical equilibrium, or “photo-stationary state.” The photolysis of NO<sub>2</sub> during the day is a direct source of tropospheric O<sub>3</sub>. The NO<sub>x</sub> concentration determines both the HO<sub>x</sub> and O<sub>3</sub> cycles. At very high concentrations, NO<sub>2</sub> can be titrated by OH, eventually leading to HNO<sub>3</sub> formation. At very low concentrations, HO<sub>2</sub> loss through self-reactions and cross reactions with RO<sub>2</sub> lead to net HO<sub>x</sub> loss. But as NO<sub>x</sub> increases, the HO<sub>2</sub>-NO reaction becomes competitive and HO<sub>2</sub> is recycled into OH increasing the chain length. Despite a short lifetime, NO<sub>x</sub> can also be transported from one place to another either in its original gaseous state or in the form of nitrates, PAN etc., and nighttime chemistry becomes important (Levy et al., 1999). In high NO<sub>x</sub> regimes like urban regions, including Delhi, the production of O<sub>3</sub> is generally limited by volatile organic compounds (VOCs). Both NO and NO<sub>2</sub> are measured at several locations in Delhi but we discuss results of NO<sub>2</sub>, here as it is observed at all the locations selected and column NO<sub>2</sub> is also measured by satellites. The change in the monthly average levels of NO<sub>2</sub> during 2020 compared to the average of 2015–2019 is shown in **Figure 9E**. While average surface NO<sub>2</sub> levels decreased by only 43% for the study sites over Delhi, the average decrease was 57, 50, 40, and 26%, respectively, for April, May, June, and July. On a different perspective, tropospheric NO<sub>2</sub> decreased by 57, 53, 32, and –6% for April, May, June, and July i.e., for the same months. The numbers are self-explanatory as April was a complete lockdown and May was a partial lockdown, while in March (average decrease of 14% only), lockdown was implemented in the last week only. The April NO<sub>2</sub> levels came down from 30 μg m<sup>-3</sup> in the previous years (2015–2019 average) to approximately 11 μg m<sup>-3</sup> in the lockdown. Because the major influence on NO<sub>2</sub> concentrations is from anthropogenic emissions, the impact of lockdown is nicely traced in surface NO<sub>2</sub> measurements. The lowest levels of NO<sub>2</sub> among the study sites are observed for NSIT-Dwarka, while the highest levels are observed for Anand Vihar in the east of Delhi. This is because NSIT-Dwarka is a more planned area with open spaces and airport, while Anand Vihar is congested with multiple emission sources. Furthermore, it is to be noted that Anand Vihar has a major inter-state bus terminal and the bus service as well as local travel is still not to full scale. Punjabi Bagh and Shadipur show almost similar patterns from 2015 to 2020, including the sudden decrease during the lockdown. The maximum change by approximately 76% is observed in April at Anand Vihar. As the lockdown is relaxed gradually, the 2020 levels start coming toward the normal. The decrease at Anand Vihar became approximately 38% in July. Levels of NO<sub>2</sub> at other locations

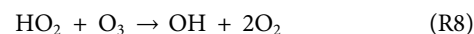
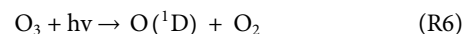
also have not come to normal levels. An early study of lockdown effect on NO<sub>2</sub> for different states of India using Aura/OMI data revealed that among the other states of India, the maximum decrease was observed over Delhi (62% over 2019 values and 54% over 2015–2019 average values) with higher decrease in phase I (25 March–14 April, 2020) compared to phase 2 (15 April–3 May, 2020) (Pathakoti et al., 2020). Similar decreases over Delhi were concluded by various studies: 63.9% (Bedi et al., 2020), 42.27% (Chhikara and Kumar, 2020), 60% (Kumari and Toshniwal, 2020), 56% (Singh et al., 2020); the differences being the varied periods for averaging as well as varying reference periods. Even in our study, in contrast to SO<sub>2</sub>, the variability of NO<sub>2</sub> among different stations exhibited an overall decrease from March to April to May to June. This indicates that as lockdown measures strengthened from March to April, people settled in their homes leading to minimum vehicular and industrial emissions, decrease in both NO<sub>2</sub> levels as well as the variability between different sites in Delhi was evident. The homogeneity between sites strengthened until May as people settled into similar patterns of life with similar patterns of emissions. This continued even in June when values started to increase with relaxations in activities, but the pattern remained similar leading to lower variability in terms of decrease in different sites in Delhi (**Figure 9E**; **Table 1**).

## O<sub>3</sub>

The daytime chemical production and loss of surface O<sub>3</sub> in the troposphere is controlled by competing reactions involving many of its precursors such as NO<sub>2</sub>, NO, CO and hydrocarbons in the presence of sunlight (Seinfeld and Pandis, 2006). It is produced by the reaction of atomic oxygen with molecular oxygen as in the stratosphere. However, this atomic oxygen does not come from the dissociation of molecular oxygen as in the stratosphere but from the dissociation of NO<sub>2</sub> as shown in the following simple reactions scheme.



OH is produced from the reaction of water with O(<sup>1</sup>D), which in turn is produced from the photolysis of O<sub>3</sub> at wavelengths <320 nm.



In the absence of competing reactions, the net effect of reactions R4, R5, and R9 is zero. The reaction of OH initiates the breakdown of CO and VOCs, resulting in the formation of RO<sub>x</sub> (e.g., R1). The simplest is HO<sub>2</sub>, formed from the oxidation of CO to CO<sub>2</sub>. While radical-radical self and cross reactions are dominant at low NO, with increasing NO<sub>x</sub>, NO

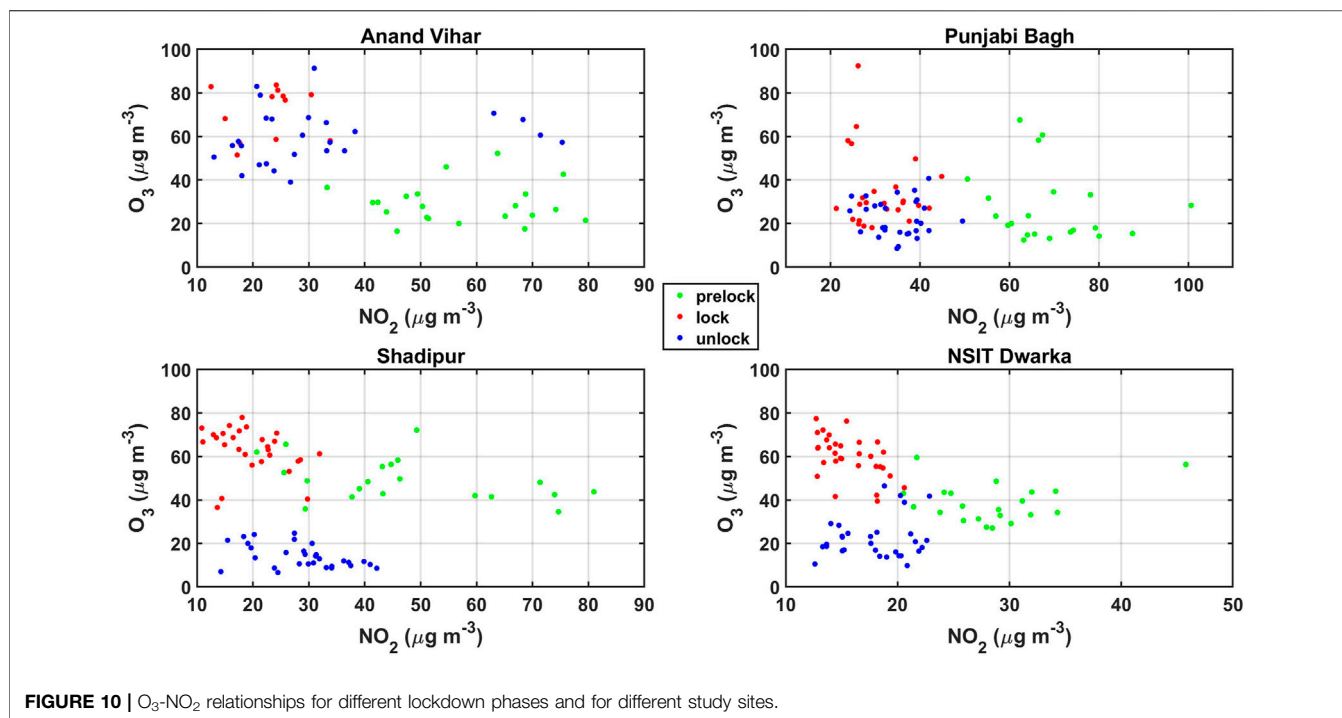
gradually outcompetes the peroxide-forming reactions, leading to rapid recycling between OH and HO<sub>2</sub>. At very high concentrations, there is net loss in the form of HNO<sub>3</sub>, while at very low concentrations of NO<sub>x</sub>, there is HO<sub>x</sub> loss in the form of peroxides. Depending on VOC to NO<sub>x</sub> ratio, the oxidation capacity increases at intermediate NO<sub>x</sub> levels. Mertens et al. (2021) employed a combination of regional chemistry climate model (CCM-COSMO) and global chemistry climate model (CCM\_EMAC) with a general circulation base model (ECHAM5) to make a sector-wise attribution of O<sub>3</sub> changes resulting out of emission reductions during the lockdown over Europe. Interestingly, the authors found that despite reduced O<sub>3</sub> production due to reduced anthropogenic emissions, the O<sub>3</sub> production efficiency (OPE) i.e., net O<sub>3</sub> production per molecule of NO<sub>x</sub> increased. It was also observed that the ratio of H<sub>2</sub>O<sub>2</sub> (HO<sub>2</sub> sink) to HNO<sub>3</sub> (OH sink) production rates exhibited an enhancement during the lockdown period indicating a shift from NO<sub>x</sub>-saturated to NO<sub>x</sub>-limited regime. Despite increased OPE, there was a net O<sub>3</sub> reduction as anthropogenic emission reduction overcompensated the enhanced OPE and natural emissions. Furthermore, as O<sub>3</sub> has a fairly long lifetime, the impact of atmospheric transport can compensate for immediate chemical changes in a region. In another study, sensitivity of global tropospheric O<sub>3</sub> burden to anthropogenic NO<sub>x</sub> reductions (COVID-2020 emission anomaly over 2010–2019) was studied employing the state-of-the-art multi-constituent satellite data assimilation system, which was used to ingest multiple satellite observations to simultaneously optimize concentrations and emissions of trace species and simulating their chemical interaction (Miyazaki et al., 2021). Strong O<sub>3</sub> response to NO<sub>x</sub> reductions in highly polluted areas attributed to NO<sub>x</sub> titrations and enhanced oxidation capacity led to local O<sub>3</sub> enhancements. The role of atmospheric transport was revealed in Miyazaki et al. study such that O<sub>3</sub> reductions in Central Eastern Eurasia were attributed to emission reductions over North America. In this study, global reductions were also estimated for peroxyacetyl nitrate (NO<sub>x</sub> reservoir) and OH. Using generalized additive models fed by reanalysis meteorological data, Ordóñez et al. (2020) showed that while NO<sub>2</sub> concentration variations in Europe were attributed to reduced emissions, O<sub>3</sub> concentration changes were mostly explained by meteorology. Over Delhi, O<sub>3</sub> reduction upto 13% was observed by Datta et al. (2021); the authors use statistical analysis to show that O<sub>3</sub> concentration variations were not explained by lockdown effects unlike PM variations, which were largely contributed by lockdown-induced emission changes.

Community Multi-Scale Air Quality (CMAQ) model estimations revealed that during lockdown, there was a 15% decrease in maximum daily 8 h average (MDA8) O<sub>3</sub> (Zhang et al., 2021). However, in some VOC-limited urban regions, O<sub>3</sub> enhancement was observed mainly due to higher reduction of NO<sub>x</sub> compared to VOCs. If both VOCs and NO<sub>x</sub> are low for example in the pristine regions, production of O<sub>3</sub> is very low. If both are high for example in a polluted urban region, high levels of O<sub>3</sub> can be produced (Seinfeld and Pandis, 2006). In the intermediate regime, O<sub>3</sub> production or loss depends upon the

levels of NO<sub>x</sub> and hydrocarbons. The transition from VOC-limited to NO<sub>x</sub>-limited regimes can be gauged through various proxies. OPE (i.e., ΔO<sub>3</sub>/ΔNO<sub>x</sub>) is a simple measure to infer the O<sub>3</sub> formation regimes with values less than 4 indicating VOC limited and greater than 7 indicating NO<sub>x</sub> limited (Wang et al., 2017). Another popular proxy is the ratio of OH-reactivity of NO<sub>x</sub> to OH-reactivity of VOC (Sinha et al., 2012). If this ratio exceeds 0.2 (±0.1), the O<sub>3</sub> production regime is VOC limited, whereas if it is below 0.01, the O<sub>3</sub> production regime is considered NO<sub>x</sub> limited. The intermediate range, 0.01 < 2 < 0.2, indicates that the peak O<sub>3</sub> production depends strongly on both NO<sub>x</sub> and VOC levels. Furthermore, as the production of HCHO is proportional to reactions of reactive organics with OH, the HCHO/NO<sub>y</sub> ratio can also be used to segregate the two regimes with 0.28 marking the transition from VOC limited to NO<sub>x</sub> limited (Sillman, 1995).

In the VOC-limited regime, decreasing VOC emissions reduces the chemical production of organic radicals (RO<sub>2</sub>), leading to decreased cycling with NO<sub>x</sub> thus reducing O<sub>3</sub> (Wang et al., 2021). In the NO<sub>x</sub>-limited regime, decreasing NO<sub>x</sub> emission reduces NO<sub>2</sub> photolysis, directly reducing O<sub>3</sub>. In contrast, in the VOC-limited regime, NO<sub>x</sub> acts to reduce O<sub>3</sub>, so decreased NO<sub>x</sub> emissions promote O<sub>3</sub> production (Kleinman, 1994). Furthermore, in the NO<sub>x</sub>-limited regime (or VOC-saturated), O<sub>3</sub> production is proportional to square root of HO<sub>x</sub> (OH + HO<sub>2</sub>) production while in the VOC-limited (or NO<sub>x</sub>-saturated) regime, O<sub>3</sub> production is directly proportional to HO<sub>x</sub> production. A WRF-Chem modelling study revealed that the IGP region (including Delhi) is in a NO<sub>x</sub> to VOC transition regime (Chutia et al., 2019). A box model study using the NCAR master mechanism found that O<sub>3</sub> production in Delhi/NCR is limited by the abundance of VOCs even though NO<sub>x</sub> is higher (Chen et al., 2021). In such VOCs-limited regimes, a decrease in NO<sub>x</sub> would lead to enhancement in O<sub>3</sub>. During the lockdown most of the vehicular emissions came to total halt except emergency vehicles. Various industries were closed as well as many other anthropogenic sources of emissions of these pollutants. However, power generation did not stop but got reduced. Major sources of NO<sub>x</sub> in Delhi are transport, industries, and diesel generator sets (Table 3). All these three sources were almost closed during the lockdown. Similarly, major sources of VOCs include transportation (~50%), brick kiln, and power plants (Guttikunda and Calori, 2013). The first two were totally closed during the lockdown. So the lockdown would lead to a much larger reduction in NO<sub>x</sub>. However, in the absence of VOC measurements over Delhi, it will be difficult to quantify the transition regions from VOC limited to NO<sub>x</sub> limited.

Surface O<sub>3</sub> shows different features at different study sites in Delhi (Figure 9F). The O<sub>3</sub> results for the Central Road Research Institute are not used here as there are often breaks in the data. One explanation for this variation is related to the ratio of VOCs to NO<sub>x</sub>. A clear increase in O<sub>3</sub> values is observed over Anand Vihar and NSIT-Dwarka, while the unlock phase brings back the O<sub>3</sub> values down. In a normal scenario, spring peak in O<sub>3</sub> is observed over Delhi as a result of biomass burning in the adjoining areas. Over Shadipur and NSIT-Dwarka, the levels had been similar before lockdown and all were showing a gradual increase from February to March. However, over



Anand Vihar and Punjabi Bagh, the increase was not gradual but there had been a decrease in the 1st week of March followed by an increase just before lockdown. However, since the onset of lockdown, O<sub>3</sub> over Anand Vihar continued to increase and daily average remained over 60 µg m<sup>-3</sup> until air masses changed in late June when O<sub>3</sub> levels started coming down. NSIT-Dwarka, located on the western part of Delhi, also showed concurrent features like Anand Vihar (east Delhi) increasing till Phase 3. However, in Phase 3, as relaxations start in transport services, the plummet in O<sub>3</sub> levels coincided exactly with an increase in NO<sub>2</sub>. This shows that during lockdown, as anthropogenic emissions decreased, O<sub>3</sub> over Delhi which is normally in a VOC-limited regime is now controlled by titration effects with NO<sub>x</sub>. The feature is specifically visible over NSIT-Dwarka, where overall NO<sub>x</sub> levels are lower among the studied sites and decreased further during lockdown (Figure 10). The O<sub>3</sub>-NO<sub>x</sub> relationships show different patterns between pre-lockdown, lockdown, and unlock periods at different sites. For instance, over Punjabi Bagh and Anand Vihar, lockdown and unlock data are indiscernible while over Shadipur and NSIT Dwarka, there is a distinct reduction in O<sub>3</sub> levels between lockdown and unlock periods. It must be mentioned here that for these O<sub>3</sub>-NO<sub>x</sub> relationships, we have not considered the variation of VOCs. However, since these are natural atmospheric data, VOCs in Figure 10, although not shown (due to nonavailability of data), would also be different for each individual point. As mentioned before from the Zhang et al. (2021) analysis, NO<sub>x</sub> reductions are likely to be much larger than VOC reductions. This is because the major sources of NO<sub>x</sub> are few and were severely impacted by the lockdown e.g., vehicular emissions but VOC sources are much more varied and all were not impacted by lockdown e.g., residential emissions.

## CONCLUSION

India started taking precaution in the initial phase of the spread of the corona virus by imposing strict lockdown from 25th March, 2020 itself. This led to closing down of all the industrial activities, all kinds of travel, educational institutes and people were asked to remain in their houses. We studied the impact of these closed anthropogenic sources of emissions during the lockdown from 25th March to almost May end and later unlocking of these till the end of July 2020 at 5 selected locations covering Delhi using *in-situ* measurements and satellite-based measurements of important pollutants. Daily and monthly average values of these pollutants for 2020 were compared with the 5-year average values from 2015 to 2019. Satellite-based measurements of monthly average AOD and tropospheric column of NO<sub>2</sub> for the entire Delhi showed changes from the 5 year average and are listed in Table 5. Comparing the average decrease of different species, it was observed that the species most affected by the lockdown as observed for April data are PM (includes both fine and coarse modes), NO<sub>2</sub> (includes both surface level and tropospheric column), and CO. In terms of percentage changes, the different species (except AOD and O<sub>3</sub>) were clumped together in April when lockdown was in full force. Overall O<sub>3</sub> showed an increase over Delhi while AOD showed a much lower decrease compared to PM. The large decrease for CO during lockdown indicates predominant contributions of anthropogenic sources in Delhi for this species. Similar decreases in both surface and columnar NO<sub>2</sub> during March-June indicate dominant contribution of surface sources to NO<sub>2</sub> columns over Delhi. While tropospheric col NO<sub>2</sub> concentrations during COVID-19 months decreased by -56.9%, -53%, and -32.4% in April, May, and June, the AOD values decreased

**TABLE 5** | Average combined percentage change for all the stations considered here as representative for changes in Delhi in monthly mean concentrations of various species during COVID-19 months with respect to average of 2015–19.

	March	April	May	June	July
AOD	10.4	-25.3	-22.5	-7.1	2.5
Tropo Col NO <sub>2</sub>	-13.4	-56.9	-53.0	-32.4	-5.5
PM <sub>10</sub>	-38.4 ± 13.2	-58.0 ± 13.6	-47.8 ± 20.8	-47.2 ± 18.2	-45.8 ± 19.1
PM <sub>2.5</sub>	-42.1 ± 11.8	-54.0 ± 17.9	-34.7 ± 19.6	35.0 ± 13.2	-33.7 ± 14.0
NO <sub>2</sub>	-14.4 ± 25.4	-56.7 ± 17.1	-49.6 ± 14.8	-39.8 ± 13.1	-25.6 ± 7.7
CO	-53.8 ± 35.6	-57.4 ± 28.5	-45.3 ± 42.6	-28.8 ± 26.3	-7.2 ± 11.0
O <sub>3</sub>	21.6 ± 46.7	43.4 ± 57.0	17.3 ± 78.3	21.4 ± 79.4	9.5 ± 82.2
SO <sub>2</sub>	-33.7 ± 32.5	-48.1 ± 4.5	-24.6 ± 24.5	-0.7 ± 30.0	20.9 ± 32.7

only by -25.3% in April, 2020 with respect to the 5 years average. These slow changes in AOD continued with -22.5% and -7.1% in May and June respectively. By July 2020, the AOD values have almost become normal. It is to be noted that AOD showed much lower decrease than tropospheric column NO<sub>2</sub>. A similar difference is also observed by Pope et al. (2018). This could be due to the fact that loss of aerosols through deposition occurs near the Earth's surface. The smaller aerosols in the boundary layer as well as in the free troposphere coagulate to form bigger particles, which also contribute to AOD. The lifetimes of aerosols near the surface are very short as mentioned in Table 4 but much longer in the free troposphere. So when emission of aerosols reduces at the surface, column values (AOD) do not change that much. However, NO<sub>2</sub> is photochemically dissociated to form NO, which is highly reactive and reacts with various gases forming nitrates as well as reforming NO<sub>2</sub>. This happens even more at the higher heights due to intense solar radiation. Hence, when the supply from the emission sources at the surface reduces, column NO<sub>2</sub> also reduces.

The *in-situ* measurements of surface level PM<sub>10</sub> and PM<sub>2.5</sub> also showed maximum decrease of -58% and -54% respectively for April, 2020. However, there was a significant decrease in March itself for both the species by -38.4% and -42.1% respectively for PM<sub>10</sub> and PM<sub>2.5</sub>. This was due to 8 days of lockdown in March coupled to seasonal change in wind direction resulting in different source regions. A decrease of -45.8% and -33.7% was observed in July also for both these species even during the second unlock phase. Also, PM<sub>10</sub> showed slightly more decrease than PM<sub>2.5</sub> in the same period. This could be because of the lifetime of PM<sub>10</sub> being shorter than PM<sub>2.5</sub> (Table 4). Decrease in NO<sub>2</sub> was almost similar to that of PM<sub>10</sub> and PM<sub>2.5</sub>. Major sources of aerosols and NO<sub>2</sub> are transport and industries (Table 3), which were totally closed during the first two phases of the lockdown. Although biogenic emissions constitute a major source of CO, large changes in CO similar to other anthropogenic markers e.g., SO<sub>2</sub> indicate overwhelming anthropogenic components in Delhi. It is to be noted that the lifetime of CO is much higher than that of SO<sub>2</sub> and other species. Singh et al. (2020) have analyzed data for the Indian region and have shown an average decrease in PM<sub>10</sub>, PM<sub>2.5</sub>, NO<sub>2</sub>, and CO by about -58%, -45%, -50%, and -38% respectively.

O<sub>3</sub>, as discussed in Section 4.6, has complex chemistry depending not only on the levels of its precursors but also on the balance of NO<sub>x</sub> and hydrocarbons. Model estimates for Delhi show that it is hydrocarbon controlled (Chen et al., 2021). We observed mixed signals (increase as well as decrease) in the levels

of O<sub>3</sub> at different locations. This could be possible due to different combinations of NO<sub>x</sub> and hydrocarbons, as these locations have different emission sources, some are heavily transport (NO<sub>x</sub>) impacted, while others have higher hydrocarbon emissions. During lockdown, as anthropogenic emissions decreased, O<sub>3</sub> over Delhi which is normally in a VOC-limited regime is now controlled by NO<sub>x</sub>. The feature is specifically visible over NSIT-Dwarka, where overall NO<sub>x</sub> levels were lower among the studied sites and decreased further during lockdown. A clear increase in O<sub>3</sub> values was observed over Anand Vihar and NSIT-Dwarka, while the unlock phase evinced a fall in the O<sub>3</sub> values. Singh et al. (2020) have found mixed variations in O<sub>3</sub> due to lockdown in different parts of India. Similar studies from China and Europe found slight increases in O<sub>3</sub> levels during the lockdown (Shi and Brasseur, 2020; Xu et al., 2020; Sicard et al., 2020).

Overall, the effect on the levels of pollutants was mainly due to the reduced vehicular emissions and atmospheric transport from the surrounding regions as well as due to power generation and other point sources. The higher peaks in PM<sub>2.5</sub> coincide with north-westerly air-masses sourced to industrial regions in Haryana and Punjab of India all the way back to Lahore in Pakistan and further back to the north-west. Simultaneously, higher levels of tropospheric NO<sub>2</sub> column values were observed in the month of May toward the north-west of Delhi and up to Pakistan in the IGP which suggests heavy pollution due to industrialization in this area acting as a source for Delhi. The ratio of decreased PM<sub>10</sub> between Punjabi Bagh and Central Road Research Institute during different months showed an average value of 1.1, which indicates a uniform impact of lockdown on PM<sub>10</sub> from north-west to south-east of urban Delhi. However for PM<sub>2.5</sub>, the ratios of Shadipur to Anand Vihar are 1.6, 1.4, 1.5, 1.7, and 1.6, respectively, for March to July months, with an average of 1.5. This near constant ratio evinces a 50% higher impact on PM<sub>2.5</sub> in Central Delhi compared to Eastern Delhi due to lockdown. It is to be noted that the lockdown was all over India. We have seen that Delhi gets affected from the surrounding regions, states, as well as even from the nearby countries such as Pakistan and Afghanistan (Figure 7). Hence, these effects are cumulative. In this context, it is worth mentioning that the control of pollution by the local government through restriction of odd-even vehicular movement (only 4 wheelers and in Delhi city only) did not yield the desired results (Chandra et al., 2018).

Hence, changes in the levels of various pollutants during the lockdown-2020 were variable depending upon the emission sources, lifetimes, and chemistry. These results are very useful

for testing and updating the emission inventories as well as for models.

## DATA AVAILABILITY STATEMENT

Publicly available datasets were analyzed in this study. This data can be found here: <https://app.cpcbcr.com/ccr/#/caaqm-dashboard/caaqm-landing/caaqm-comparison-data>.

## AUTHOR CONTRIBUTIONS

CM: conceptualization, overall data analysis, review and write-up. HG: FlexPart and AOD data analysis, review and write-up. SL: conceptualization, overall data analysis, review and write-up. RKY: NO<sub>2</sub> columnar data analysis, review and editing. RB: data analysis, review and editing. TD: data analysis, review and editing.

## REFERENCES

- Andrews, M., Areekal, B., Rajesh, K., Krishnan, J., Suryakala, R., Krishnan, B., et al. (2020). First Confirmed Case of COVID-19 Infection in India: A Case Report. *Indian J. Med. Res.* 151 (5), 490–492. doi:10.4103/ijmr.IJMR\_2131\_20
- Apte, J. S., Marshall, J. D., Cohen, A. J., and Brauer, M. (2015). Addressing Global Mortality from Ambient PM<sub>2.5</sub>. *Environ. Sci. Technol.* 49 (13), 8057–8066. doi:10.1021/acs.est.5b01236
- ARAI and TERI (2018). Executive Summary: Source Apportionment of PM<sub>2.5</sub> & PM<sub>10</sub> of Delhi NCR for Identification of Major Sources. Report No. ARAI/16-17/DHI-SA-NCR/Exec\_Summ. Available at: <https://www.teriin.org/sites/default/files/2018-08/Exec-summary.pdf>
- Bali, K., Dey, S., Ganguly, D., and Smith, K. R. (2019). Space-time Variability of Ambient PM<sub>2.5</sub> Diurnal Pattern over India from 18-years (2000–2017) of MERRA-2 Reanalysis Data. *Atmos. Chem. Phys. Discuss.*, 1–23. doi:10.5194/acp-2019-731
- Bangar, V., Mishra, A. K., Jangid, M., and Rajput, P. (2021). Elemental Characteristics and Source-Apportionment of PM<sub>2.5</sub> during the Post-monsoon Season in Delhi, India. *Front. Sustain. Cities* 3, 648551. doi:10.3389/frsc.2021.648551
- Bedi, J. S., Dhaka, P., Vijay, D., Aulakh, R. S., and Gill, J. P. S. (2020). Assessment of Air Quality Changes in the Four Metropolitan Cities of India during COVID-19 Pandemic Lockdown. *Aerosol Air Qual. Res.* 20, 2062–2070. doi:10.4209/aaqr.2020.05.0209
- Beig, G., Srinivas, R., Parkhi, N. S., Carmichael, G. R., Singh, S., Sahu, S. K., et al. (2019). Anatomy of the winter 2017 Air Quality Emergency in Delhi. *Sci. Total Environ.* 681, 305–311. doi:10.1016/j.scitotenv.2019.04.347
- Bithal, S. (2018). Delhi Loses 80 Lives to Air Pollution Every Day, Says Study: Outdoor Air Pollution Is the Fifth Largest Killer in India, Down to Earth published on, <https://www.downtoearth.org.in/news/delhi-loses-80-lives-to-air-pollution-every-day-says-study-50222> (Accessed 10 Dec 2018).
- Chandra, B. P., Sinha, V., Hakkim, H., Kumar, A., Pawar, H., Mishra, A. K., et al. (2018). Odd-even Traffic Rule Implementation during winter 2016 in Delhi Did Not Reduce Traffic Emissions of VOCs, Carbon Dioxide, Methane and Carbon Monoxide. *Curr. Sci.* 114 (6), 1318–1325. doi:10.18520/cs/v114/i06/1318-1325
- Chen, Y., Beig, G., Archer-Nicholls, S., Drysdale, W., Acton, W. J. F., Lowe, D., et al. (2021). Avoiding High Ozone Pollution in Delhi, India. *Faraday Discuss.* 226, 502–514. doi:10.1039/D0FD00079E
- Chhikara, A., and Kumar, N. (2020). COVID-19 Lockdown: Impact on Air Quality of Three Metro Cities in India. *ajae* 14 (4), 378–393. doi:10.5572/ajae.2020.14.4.378
- Chutia, L., Ojha, N., Girach, I. A., Sahu, L. K., Alvarado, L. M. A., Burrows, J. P., et al. (2019). Distribution of Volatile Organic Compounds over Indian Subcontinent during winter: WRF-Chem Simulation versus Observations. *Environ. Pollut.* 252, 256–269. doi:10.1016/j.envpol.2019.05.097

## ACKNOWLEDGMENTS

We acknowledge that OMI NO<sub>2</sub> column data were downloaded from <https://disc.gsfc.nasa.gov/>. VIIRS AOD data were downloaded from <https://ladsweb.modaps.eosdis.nasa.gov/>. The reanalysis data of meteorology were downloaded from <https://rda.ucar.edu/datasets/ds083.2/>. Authors thank science teams and personnel associated with generating these data. The FLEXPART model was downloaded from <https://www.flexpart.eu/>. Authors thank developers and scientists associated with FLEXPART model development. SL is grateful to the Director PRL, Ahmedabad and to CSIR, New Delhi for their support for his position. TD and RB are grateful to Director CSIR-IMMT, Bhubaneswar for support and ISRO-GBP (ATCTM) for funding. Authors sincerely thank the two reviewers for their constructive comments that has improved the MS to its present form. We also thank the editor for quick and timely processing of the MS.

- Conibear, L., Butt, E. W., Knote, C., Arnold, S. R., and Spracklen, D. V. (2018). Residential Energy Use Emissions Dominate Health Impacts from Exposure to Ambient Particulate Matter in India. *Nat. Commun.* 9, 617. doi:10.1038/s41467-018-02986-7
- Conley, S. A., Faloona, I. C., Lenschow, D. H., Campos, T., Heizer, C., Weinheimer, A., et al. (2011). A Complete Dynamical Ozone Budget Measured in the Tropical marine Boundary Layer during PASE. *J. Atmos. Chem.* 68, 55–70. doi:10.1007/s10874-011-9195-0
- Croft, B., Pierce, J. R., and Martin, R. V. (2014). Interpreting Aerosol Lifetimes Using the GEOS-Chem Model and Constraints from Radionuclide Measurements. *Atmos. Chem. Phys.* 14, 4313–4325. doi:10.5194/acp-14-4313-2014
- Datta, A., Rahman, M. H., and Suresh, R. (2021). Did the COVID-19 Lockdown in Delhi and Kolkata Improve the Ambient Air Quality of the Two Cities? *J. Environ. Qual.* 50 (2), 485–493. doi:10.1002/jeq2.20192Epub 2021 Jan 25
- Dhaka, S. K., Chetna, V. K., Dimri, A. P., Singh, N., et al. (2020). PM<sub>2.5</sub> Diminution and Haze Events over Delhi during the COVID-19 Lockdown Period: an Interplay between the Baseline Pollution and Meteorology. *Sci. Rep.* 10, 13442. doi:10.1038/s41598-020-70179-8
- Gadhavi, H. S., Renuka, K., Kiran, V. R., Jayaraman, A., Stohl, A., Klimont, Z., et al. (2015). Evaluation of black carbon emission inventories using a Lagrangian dispersion model a case study over southern India. *Atmos. Chem. Phys.* 15, 1447–1461. doi:10.5194/acp-15-1447-2015
- Goel, V., Hazarika, N., Kumar, M., Singh, V., Thamban, N. M., and Tripathi, S. N. (2021). Variations in Black Carbon Concentration and Sources during COVID-19 Lockdown in Delhi. *Chemosphere* 270, 129435. doi:10.1016/j.chemosphere.2020.129435
- Grythe, H., Kristiansen, N. I., Groot Zwaafink, C. D., Eckhardt, S., Ström, J., Tunved, P., et al. (2017). A New Aerosol Wet Removal Scheme for the Lagrangian Particle Model FLEXPART V10. *Geosci. Model. Dev.* 10, 1447–1466. doi:10.5194/gmd-10-1447-2017
- Guttikunda, S. K., and Calori, G. (2013). A GIS Based Emissions Inventory at 1 Km × 1 Km Spatial Resolution for Air Pollution Analysis in Delhi, India. *Atmos. Environ.* 67, 101–111. doi:10.1016/j.atmosenv.2012.10.040
- Hama, S. M. L., Kumar, P., Harrison, R. M., Bloss, W. J., Khare, M., Mishra, S., et al. (2020). Four-year Assessment of Ambient Particulate Matter and Trace Gases in the Delhi-NCR Region of India. *Sust. Cities Soc.* 54, 102003. doi:10.1016/j.scs.2019.102003
- Inomata, Y., Iwasaka, Y., Osada, K., Hayashi, M., Mori, I., Kido, M., et al. (2006). Vertical Distributions of Particles and Sulfur Gases (Volatile Sulfur Compounds and SO<sub>2</sub>) over East Asia: Comparison with Two Aircraft-Borne Measurements under the Asian Continental Outflow in Spring and Winter. *Atmos. Environ.* 40, 430–444. doi:10.1016/j.atmosenv.2005.09.055
- Jain, S., Sharma, S. K., Vijayan, N., and Mandal, T. K. (2020). Seasonal Characteristics of Aerosols (PM<sub>2.5</sub> and PM<sub>10</sub>) and Their Source

- Apportionment Using PMF: A Four Year Study over Delhi, India. *Environ. Pollut.* 262, 114337. doi:10.1016/j.envpol.2020.114337
- Jain, S., and Sharma, T. (2020). Social and Travel Lockdown Impact Considering Coronavirus Disease (COVID-19) on Air Quality in Megacities of India: Present Benefits, Future Challenges and Way Forward. *Aerosol Air Qual. Res.* 20 (6), 1222–1236. doi:10.4209/aaqr.2020.04.0171
- Jaiprakash, S. A., Habib, G., Raman, R., and Gupta, T. (2017). Chemical characterization of PM<sub>1</sub> aerosol in Delhi and source apportionment using positive matrix factorization. *Environ. Sci. Pollut. Res.* 24, 445–462. doi:10.1007/s11356-016-7708-8
- Kleinman, L. I. (1994). Low and High NO<sub>x</sub> Tropospheric Photochemistry. *J. Geophys. Res.* 99, 16831–16838. doi:10.1029/94jd01028
- Kristiansen, N. I., Stohl, A., Olivieri, D. J. L., Croft, B., Søvdø, O. A., Klein, H., et al. (2016). Evaluation of Observed and Modelled Aerosol Lifetimes Using Radioactive Tracers of Opportunity and an Ensemble of 19 Global Models. *Atmos. Chem. Phys.* 16, 3525–3561. doi:10.5194/acp-16-3525-2016
- Krotkov, N. A., Lamsal, L. N., Marchenko, S. V., Bucselá, E. J., and Swartz, W. H. (2019). *OMI/Aura Nitrogen Dioxide (NO<sub>2</sub>) Total and Tropospheric Column 1-orbit L2 Swath 13x24 Km V003*. Greenbelt, MD, USA: Goddard Earth Sciences Data and Information Services Center (GES DISC). Joiner, J. and the OMI core team. doi:10.5067/Aura/OMI/DATA2017
- Kumari, P., and Toshniwal, D. (2020). Impact of Lockdown Measures during COVID-19 on Air Quality- A Case Study of India. *Int. J. Environ. Health Res.* 00 (00), 1–8. doi:10.1080/09603123.2020.1778646
- Lalchandani, V., Kumar, V., Tobler, A., M. Thamban, N., Mishra, S., Slowik, J. G., et al. (2021). Real-time Characterization and Source Apportionment of fine Particulate Matter in the Delhi Megacity Area during Late winter. *Sci. Total Environ.* 770, 145324. doi:10.1016/j.scitotenv.2021.145324
- Lamsal, L. N., Krotkov, N. A., Vasilkov, A., Marchenko, S., Qin, W., Yang, E.-S., et al. (2020). OMI/Aura Nitrogen Dioxide Standard Product with Improved Surface and Cloud Treatments. *Atmos. Meas. Tech.* 14 (1), 455–479. doi:10.5194/amt-2020-200
- Lawrence, M. G., and Lelieveld, J. (2010). Atmospheric pollutant outflow from southern Asia: a review. *Atmos. Chem. Phys.* 10, 11017–11096. doi:10.5194/acp-10-11017-2010
- Le, T., Wang, Y., Liu, L., Yang, J., Yung, Y. L., Li, G., et al. (2020). Unexpected Air Pollution with Marked Emission Reductions during the COVID-19 Outbreak in China. *Science* 369 (6504), 702–706. doi:10.1126/science.abb7431
- Lee, C., Richter, A., Lee, H., Kim, Y. J., Burrows, J. P., Lee, Y. G., et al. (2008). Impact of Transport of Sulfur Dioxide from the Asian Continent on the Air Quality over Korea during May 2005. *Atmos. Environ.* 42, 1461–1475. doi:10.1016/j.atmosenv.2007.11.006
- Lelieveld, J., Evans, J. S., Fnais, M., Giannadaki, D., and Pozzer, A. (2015). The contribution of outdoor air pollution sources to premature mortality on a global scale. *Nature* 525, 367–371. doi:10.1038/nature15371
- Levelt, P. F., Van Den Oord, G. H. J., Dobber, M. R., Malkki, A., Visser, H., Vries, J., et al. (2006). The Ozone Monitoring Instrument. *IEEE Trans. Geosci. Remote Sensing* 44, 1093–1101. doi:10.1109/tgrs.2006.872333
- Levy, H., II, Moxim, W. J., Klonecki, A. A., and Kasibhatla, P. S. (1999). Simulated Tropospheric NO<sub>x</sub>: Its Evaluation, Global Distribution and Individual Source Contributions. *J. Geophys. Res.* 104, 26279–26306. doi:10.1029/1999JD900442
- Levy, R. C., Mattoo, S., Sawyer, V., and Munchak, L. A. (2020). *AERDT\_L2\_VIIRS\_SNPP - VIIRS/SNPP Dark Target Aerosol L2 6-Min Swath 6 Km*. accessed on: 2020-09-01. doi:10.5067/VIIRS/AERDT\_L2\_VIIRS\_SNPP.001
- Levy, R. C., Munchak, L. A., Mattoo, S., Patadia, F., Remer, L. A., and Holz, R. E. (2015). Towards a Long-Term Global Aerosol Optical Depth Record: Applying a Consistent Aerosol Retrieval Algorithm to MODIS and VIIRS-Observed Reflectance. *Atmos. Meas. Tech.* 8, 4083–4110. doi:10.5194/amt-8-4083-2015
- Liu, F., Beirle, S., Zhang, Q., Dörner, S., He, K., and Wagner, T. (2016). NO<sub>x</sub> Lifetimes and Emissions of Cities and Power Plants in Polluted Background Estimated by Satellite Observations. *Atmos. Chem. Phys.* 16, 5283–5298. doi:10.5194/acp-16-5283-2016
- Mahato, S., Pal, S., and Ghosh, K. G. (2020). Effect of Lockdown amid COVID-19 Pandemic on Air Quality of the Megacity Delhi, India. *Sci. Total Environ.* 730, 139086. doi:10.1016/j.scitotenv.2020.139086
- Mallik, C., and Lal, S. (2011). Changing Long-Term Trends in Tropospheric Temperature over Two Megacities in the Indo-Gangetic Plain. *Curr. Sci.* 101 (5), 637–644.
- Mallik, C., Venkataramani, S., and Lal, S. (2015). Trace gases over a semi-arid urban site in western India: variability and inter-correlations. *J. Atmos. Chem.* 72, 143–164. doi:10.1007/s10874-015-9311-7
- Mallik, C., Chandra, N., Venkataramani, S., and Lal, S. (2016). Variability of Atmospheric Carbonyl Sulfide at a Semi-arid Urban Site in Western India. *Sci. Total Environ.* 551–552, 725–737. doi:10.1016/j.scitotenv.2016.02.014
- Mertens, M., Jöckel, P., Matthes, S., Nützel, M., Grewe, V., and Sausen, R. (2021). COVID-19 Induced Lower-Tropospheric Ozone Changes. *Environ. Res. Lett.* 16 (6), 064005. doi:10.1088/1748-9326/abf191
- Miyazaki, K., Bowman, K., Sekiya, T., Takigawa, M., Neu, J. L., Sudo, K., et al. (2021). Global Tropospheric Ozone Responses to Reduced NO<sub>x</sub> Emissions Linked to the COVID-19 Worldwide Lockdowns. *Sci. Adv.* 7, eabf7460, 2021. 09 Jun 2021. doi:10.1126/sciadv.abf7460
- Monks, P. S., Archibald, A. T., Colette, A., Cooper, O., Coyle, M., Derwent, R., et al. (2015). Tropospheric Ozone and its Precursors From the Urban to the Global Scale From Air Quality to Short-Lived Climate Forcer. *Atmos. Chem. Phys.* 15, 8889–8973. doi:10.5194/acp-15-8889-2015
- Nagar, P. K., Singh, D., Sharma, M., Kumar, A., Aneja, V. P., George, M. P., et al. (2015). Characterization of PM<sub>2.5</sub> in Delhi: role and impact of secondary aerosol, burning of biomass, and municipal solid waste and crustal matter. *Environ. Sci. Pollut. Res.* 24, 25179–25189. doi:10.1007/s11356-017-0171-3
- Nath, J., Panda, S., Patra, S. S., Ramasamy, B., and Das, T. (2021). Variation of Black Carbon and Particulate Matter in Bhubaneswar during the Pre-monsoon: Possible Impact of Meteorology and COVID-19 Lockdown. *Curr. Sci.* 120 (2), 313–321. doi:10.18520/cs/v120/i2/313-321
- National Centers for Environmental Prediction (NCEP)/National Weather Service/NOAA/U.S. Department of Commerce (2000). *Research Data Archive at the National Center for Atmospheric Research*. Boulder, CO: Computational and Information Systems Laboratory. updated daily. NCEP FNL Operational Model Global Tropospheric Analyses, continuing from July 1999. doi:10.5065/D6M043C6(Accessed Sep 01, 2020)
- Navas, M. J., Jiménez, A. M., and Galán, G. (1997). Air Analysis: Determination of Nitrogen Compounds by Chemiluminescence. *Atmos. Environ.* 31 (3), 603–608. doi:10.1016/s1352-2310(97)00153-2
- Nedelec, P., Cammas, J.-P., Thouret, V., Athier, G., Cousin, J.-M., Legrand, C., et al. (2003). An Improved Infrared Carbon Monoxide Analyser for Routine Measurements Aboard Commercial Airbus Aircraft: Technical Validation and First Scientific Results of the MOZAIC III Programme. *Atmos. Chem. Phys.* 3, 1551–1564. doi:10.5194/acp-3-1551-2003
- Ordóñez, C., Garrido-Perez, J. M., and García-Herrera, R. (2020). Early spring Near-Surface Ozone in Europe during the COVID-19 Shutdown: Meteorological Effects Outweigh Emission Changes. *Sci. Total Environ.* 747, 141322. doi:10.1016/j.scitotenv.2020.141322
- Panda, S., Mallik, C., Nath, J., Das, T., and Ramasamy, B. (2021). A Study on Variation of Atmospheric Pollutants over Bhubaneswar during Imposition of Nationwide Lockdown in India for the COVID-19 Pandemic. *Air Qual. Atmos. Health* 14, 97–108. doi:10.1007/s11869-020-00916-5
- Pandithurai, G., Dipu, S., Dani, K. K., Tiwari, S., Bisht, D. S., Devara, P. C. S., et al. (2008). Aerosol Radiative Forcing during Dust Events over New Delhi, India. *J. Geophys. Res.* 113, 26279–26306. doi:10.1029/2008JD009804
- Pathakoti, M., Muppalla, A., Hazra, S., Dangeti, M., Shekhar, R., Jella, S., et al. (2020). An Assessment of the Impact of a Nation-wide Lockdown on Air Pollution - a Remote Sensing Perspective over India. *Atmos. Chem. Phys.* 2020, 1–16. doi:10.5194/acp-2020-621
- Perrino, C., Tiwari, S., Catrambone, M., Torre, S. D., Rantica, E., and Canepari, S. (2011). Chemical Characterization of Atmospheric PM in Delhi, India, during Different Periods of the Year Including Diwali Festival. *Atmos. Pollut. Res.* 2 (4), 418–427. doi:10.5094/APR.2011.048
- Pisso, I., Sollum, E., Grythe, H., Kristiansen, N. I., Cassiani, M., Eckhardt, S., et al. (2019). The Lagrangian Particle Dispersion Model FLEXPART Version 10.4. *Geosci. Model. Dev.* 12, 4955–4997. doi:10.5194/gmd-12-4955-2019
- Pope, R. J., Arnold, S. R., Chipperfield, M. P., Latter, B. G., Siddans, R., and Kerridge, B. J. (2018). Widespread Changes in UK Air Quality Observed from Space. *Atmos. Sci. Lett.* 19, e817. doi:10.1002/asl.817

- Rahaman, S., Jahangir, S., Chen, R., Kumar, P., and Thakur, S. (2021). COVID-19's Lockdown Effect on Air Quality in Indian Cities Using Air Quality Zonal Modeling. *Urban Clim.* 36, 100802. doi:10.1016/j.uclim.2021.100802
- Ranjan, A. K., Patra, A. K., and Gorai, A. K. (2020). Effect of lockdown due to SARS COVID-19 on aerosol optical depth (AOD) over urban and mining regions in India. *Sci. Total Environ.* 745, 141024. doi:10.1016/j.scitotenv.2020.141024
- Rajput, P., Sarin, M., Sharma, D., and Singh, D. (2014). Characteristics and Emission Budget of Carbonaceous Species from post-harvest Agricultural-Waste Burning in Source Region of the Indo-Gangetic Plain. *Tellus B: Chem. Phys. Meteorology* 66 (1), 21026. doi:10.3402/tellusb.v66.21026
- Rastogi, N., Singh, A., Singh, D., and Sarin, M. M. (2014). Chemical characteristics of PM<sub>2.5</sub> at a source region of biomass burning emissions: Evidence for secondary aerosol formation. *Environ. Pollut.* 184, 563–569. doi:10.1016/j.envpol.2013.09.037
- Reddington, C. L., Conibear, L., Knute, C., Silver, B. J., Li, Y. J., Chan, C. K., et al. (2019). Exploring the Impacts of Anthropogenic Emission Sectors on PM<sub>2.5</sub> and Human Health in South and East Asia. *Atmos. Chem. Phys.* 19 (18), 11887–11910. doi:10.5194/acp-19-11887-2019
- Renuka, K., Gadhavi, H., Jayaraman, A., Rao, S., and Lal, S. (2020). Study of mixing ratios of SO<sub>2</sub> in a tropical rural environment in south India. *J. Earth Sys. Sci.* 129 (104). doi:10.1007/s12040-020-1366-4
- Sahu, S. K., Beig, G., and Parkhi, N. (2015). High Resolution Emission Inventory of NO<sub>x</sub> and CO for Mega City Delhi, India. *Aerosol Air Qual. Res.* 15, 1137–1144. doi:10.4209/aaqr.2014.07.0132
- Sawyer, V., Levy, R. C., Mattoo, S., Cureton, G., Shi, Y., and Remer, L. A. (2020). Continuing the MODIS Dark Target Aerosol Time Series with VIIRS. *Remote Sensing* 12, 308. doi:10.3390/rs12020308
- Seibert, P., and Frank, A. (2004). Source-receptor Matrix Calculation with a Lagrangian Particle Dispersion Model in Backward Mode. *Atmos. Chem. Phys.* 4, 51–63. doi:10.5194/acp-4-51-2004
- Seinfeld, J. H., and Pandis, S. N. (2006). *Atmospheric Chemistry and Physics: From Air Pollution to Climate Change*. John Wiley & Sons.
- Shah, V., Jacob, D. J., Li, K., Silvern, R. F., Zhai, S., Liu, M., et al. (2020). Effect of Changing NO<sub>x</sub> Lifetime on the Seasonality and Long-Term Trends of Satellite-Observed Tropospheric NO<sub>2</sub> Columns over China. *Atmos. Chem. Phys.* 20, 1483–1495. doi:10.5194/acp-20-1483-2020
- Sharma, S. K., Sharma, A., Saxena, M., Choudhary, N., Masiwal, R., Mandal, T. K., et al. (2016). Chemical Characterization and Source Apportionment of Aerosol at an Urban Area of Central Delhi, India. *Atmos. Pollut. Res.* 7 (1), 110–121. doi:10.1016/j.apr.2015.08.002
- Shi, X., and Brasseur, G. P. (2020). The response in air quality to the reduction of Chinese economic activities during the COVID-19 outbreak. *Geophys. Res. Lett.* 47, e2020GL088070. doi:10.1029/2020GL088070
- Sicard, P., De Marco, A., Agathokleous, E., Feng, Z., Xu, X., Paoletti, E., et al. (2020). Amplified Ozone Pollution in Cities during the COVID-19 Lockdown. *Sci. Total Environ.* 735, 139542. doi:10.1016/j.scitotenv.2020.139542
- Sillman, S. (1995). The Use of NO<sub>y</sub>, H<sub>2</sub>O<sub>2</sub>, and HNO<sub>3</sub> as Indicators for Ozone-NO<sub>x</sub>-Hydrocarbon Sensitivity in Urban Locations. *J. Geophys. Res.* 100, 14175–14188. doi:10.1029/94jd02953
- Sindhvani, R., Goyal, P., Kumar, S., and Kumar, A. (2015). Anthropogenic Emission Inventory of Criteria Air Pollutants of an Urban Agglomeration - National Capital Region (NCR), Delhi. *Aerosol Air Qual. Res.* 15, 1681–1697. doi:10.4209/aaqr.2014.11.0271
- Singh, G. K., Choudhary, V., Rajeev, P., Paul, D., and Gupta, T. (2021). Understanding the Origin of Carbonaceous Aerosols during Periods of Extensive Biomass Burning in Northern India. *Environ. Pollut.* 270, 116082. doi:10.1016/j.envpol.2020.116082
- Singh, V., Singh, S., Biswal, A., Kesarkar, A. P., Mor, S., and Ravindra, K. (2020). Diurnal and Temporal Changes in Air Pollution during COVID-19 Strict Lockdown over Different Regions of India. *Environ. Pollut.* 266, 115368. doi:10.1016/j.envpol.2020.115368
- Sinha, V., Williams, J., Diesch, J. M., Drewnick, F., Martinez, M., Harder, H., et al. (2012). Constraints on Instantaneous Ozone Production Rates and Regimes during DOMINO Derived Using *In-Situ* OH Reactivity Measurements. *Atmos. Chem. Phys.* 12, 7269–7283. doi:10.5194/acp-12-7269-2012
- Stevenson, D. S., Dentener, F. J., Schultz, M. G., Ellingsen, K., van Noije, T. P. C., Wild, O., et al. (2006). Multimodel Ensemble Simulations of Present-Day and Near-Future Tropospheric Ozone. *J. Geophys. Res.* 111, D08301. doi:10.1029/2005JD006338
- Textor, C., Schulz, M., Guibert, S., Kinne, S., Balkanski, Y., Bauer, S., et al. (2006). Analysis and Quantification of the Diversities of Aerosol Life Cycles within AeroCom. *Atmos. Chem. Phys.* 6, 1777–1813. doi:10.5194/acp-6-1777-2006
- Wang, T., Xue, L., Brimblecombe, P., Lam, Y. F., Li, L., and Zhang, L. (2017). Ozone Pollution in China: A Review of Concentrations, Meteorological Influences, Chemical Precursors, and Effects. *Sci. Total Environ.* 575, 1582–1596. doi:10.1016/j.scitotenv.2016.10.081
- Wang, W., van der A, R., Ding, J., van Weele, M., and Cheng, T. (2021). Spatial and Temporal Changes of the Ozone Sensitivity in China Based on Satellite and Ground-Based Observations. *Atmos. Chem. Phys.* 21, 7253–7269. doi:10.5194/acp-21-7253-2021
- Williams, J. E., Weele, M. V., Velthoven, P. F. J. v., Scheele, M. P., Liousse, C., and Werf, G. R. v. d. (2012). The Impact of Uncertainties in African Biomass Burning Emission Estimates on Modeling Global Air Quality, Long Range Transport and Tropospheric Chemical Lifetimes. *Atmosphere* 3 (1), 132–163. doi:10.3390/atmos3010132
- Xu, K., Cui, K., Young, L.-H., Hsieh, Y.-K., Wang, Y.-F., Zhang, J., et al. (2020). Impact of the COVID-19 Event on Air Quality in Central China. *Aerosol Air Qual. Res.* 20, 915–929. doi:10.4209/aaqr.2020.04.0150
- Young, P. J., Archibald, A. T., Bowman, K. W., Lamarque, J.-F., Naik, V., Stevenson, D. S., et al. (2013). Pre-industrial to End 21st century Projections of Tropospheric Ozone from the Atmospheric Chemistry and Climate Model Intercomparison Project (ACCMIP). *Atmos. Chem. Phys.* 13, 2063–2090. doi:10.5194/acp-13-2063-2013
- Zhang, M., Katiyar, A., Zhu, S., Shen, J., Xia, M., Ma, J., et al. (2021). Impact of Reduced Anthropogenic Emissions during COVID-19 on Air Quality in India. *Atmos. Chem. Phys.* 21, 4025–4037. doi:10.5194/acp-21-4025-2021

**Conflict of Interest:** The authors declare that the research was conducted in the absence of any commercial or financial relationships that could be construed as a potential conflict of interest.

**Publisher's Note:** All claims expressed in this article are solely those of the authors and do not necessarily represent those of their affiliated organizations, or those of the publisher, the editors and the reviewers. Any product that may be evaluated in this article, or claim that may be made by its manufacturer, is not guaranteed or endorsed by the publisher.

Copyright © 2021 Mallik, Gadhavi, Lal, Yadav, Boopathy and Das. This is an open-access article distributed under the terms of the Creative Commons Attribution License (CC BY). The use, distribution or reproduction in other forums is permitted, provided the original author(s) and the copyright owner(s) are credited and that the original publication in this journal is cited, in accordance with accepted academic practice. No use, distribution or reproduction is permitted which does not comply with these terms.